

# 1 Steamed broccoli sprouts alleviate gut inflammation and 2 retain gut microbiota against DSS-induced symptoms.

3  
4 Johanna M. Holman<sup>1</sup>, Louisa Colucci<sup>2</sup>, Dorien Baudewyns<sup>3</sup>, Joe Balkan<sup>4</sup>, Timothy Hunt<sup>5</sup>,  
5 Benjamin Hunt<sup>5</sup>, Lola Holcomb<sup>6</sup>, Grace Chen<sup>7</sup>, Peter L. Moses<sup>8,9</sup>, Gary M. Mawe<sup>8</sup>, Tao Zhang<sup>10</sup>,  
6 Yanyan Li<sup>1\*</sup>, Suzanne L. Ishaq<sup>1\*</sup>

7  
8

9 <sup>1</sup> School of Food and Agriculture, University of Maine, Orono, Maine, USA 04469

10 <sup>2</sup> Department of Biology, Husson University, Bangor, Maine, USA 04401

11 <sup>3</sup> Department of Psychology, University of Maine, Orono, USA 04469

12 <sup>4</sup> Department of Chemical and Biological Engineering, Tufts University, Medford,  
13 Massachusetts, USA 02155

14 <sup>5</sup> Department of Biology, University of Maine, Orono, Maine, USA 04469

15 <sup>6</sup> Graduate School of Biomedical Sciences and Engineering, University of Maine, Orono, Maine,  
16 USA 04469

17 <sup>7</sup> Department of Internal Medicine, University of Michigan Medical School, Ann Arbor,  
18 Michigan, USA 48109

19 <sup>8</sup> Departments of Neurological Sciences and of Medicine, Larner College of Medicine,  
20 University of Vermont, Burlington, Vermont, USA 05401

21 <sup>9</sup> Finch Therapeutics, Somerville, Massachusetts, USA 02143

22 <sup>10</sup> School of Pharmacy and Pharmaceutical Sciences, SUNY Binghamton University, Johnson  
23 City, New York, USA 13790

24  
25  
26 **\*Corresponding authors:**  
27 Suzanne L. Ishaq, University of Maine, School of Food and Agriculture, Orono, ME 04469,  
28 [sue.ishaq@maine.edu](mailto:sue.ishaq@maine.edu), 1-207-581-2770  
29 Yanyan Li, University of Maine, School of Food and Agriculture, Orono, ME 04469,  
30 [yanyan.li@maine.edu](mailto:yanyan.li@maine.edu), 1-207-581-3134  
31

32 **Keywords:** inflammatory bowel disease, ulcerative colitis, broccoli, broccoli sprouts,  
33 sulforaphane, glucoraphanin, gut microbiota, dietary bioactives.

34

35 **Abstract:** Inflammatory Bowel Diseases (IBD) are devastating conditions of the gastrointestinal  
36 tract with limited treatments, and dietary intervention may be effective, affordable, and safe for  
37 managing symptoms. Ongoing research has identified inactive compounds in broccoli sprouts, like  
38 glucoraphanin, and that mammalian gut microbiota play a role in metabolizing it to the anti-  
39 inflammatory sulforaphane. The biogeographic location of participating microbiota and how that  
40 affects anti-inflammatory benefits to the host is unknown. We fed specific pathogen free C57BL/6  
41 mice either a control diet or a 10% steamed broccoli sprout diet, and gave a three-cycle regimen  
42 of 2.5% dextran sodium sulfate (DSS) in drinking water over a 34-day experiment to simulate  
43 chronic, relapsing ulcerative colitis. We monitored body weight, fecal characteristics, lipocalin,  
44 and bacterial communities from the contents and mucosa in the jejunum, cecum, and colon. Mice  
45 fed the broccoli sprout diet while receiving DSS performed better than mice fed the control diet  
46 while receiving DSS for all disease parameters, including significantly more weight gain, lower  
47 Disease Activity Index scores, lower serum lipocalin, and higher bacterial richness in all gut  
48 locations. Bacterial communities were assorted by gut location except in the mice receiving the  
49 control diet and DSS treatment. Importantly, our results suggested that broccoli sprout feeding  
50 effectively abrogated the effects of DSS on gut microbiota, as bacterial communities were similar  
51 between mice receiving broccoli sprouts with and without DSS. Collectively, these results strongly  
52 support the protective effect of steamed broccoli sprouts against gut microbiota dysbiosis and  
53 development of colitis induced by DSS.

54

55 **Importance:** Spatially resolved microbial communities provide greater insight than fecal  
56 microbial communities when investigating host-microbe interactions. Here, we show that a 10%  
57 broccoli sprout diet protects mice from the negative effects of dextran sodium sulfate induced

58 colitis, that colitis erases biogeographical patterns of bacterial communities in the gut, and that the  
59 cecum is not likely to be a significant contributor to colonic bacteria of interest in the DSS mouse  
60 model of ulcerative colitis. Mice fed the broccoli sprout diet while receiving DSS performed better  
61 than mice fed the control diet while receiving DSS for all disease parameters, including  
62 significantly more weight gain, lower Disease Activity Index scores. Broccoli sprouts represent an  
63 affordable, accessible, and safe method of resolving DSS-induced inflammation and colitis.  
64 Information on how the gut microbiome mediates health benefits is critical to making effective  
65 medical recommendations.

66

## 67 **Introduction**

68 Inflammatory Bowel Diseases (IBD) are globally prevalent, chronic inflammatory diseases  
69 of multifactorial origin with an annual healthcare cost of billions of dollars in the United States  
70 alone (1, 2). IBD occurs in the gastrointestinal tract, and can be accompanied by autoimmune  
71 dysfunction, leading to microbial community changes in the gut. In addition to being chronic and  
72 debilitating, a longer duration of IBD is associated with an increased risk of developing  
73 gastrointestinal cancers such as colorectal cancer (3–6). Treatments are currently limited to  
74 alleviating inflammatory symptoms, and returning patients to as close to homeostasis as possible.  
75 Diet can play an important role in the management of IBD as a source of anti-inflammatory  
76 metabolites, and as a tool for influencing the robustness of gut microbiomes. However, many  
77 guidelines for IBD patients recommend avoiding sulfur-rich foods which produce metabolites that  
78 might exacerbate symptoms in the gut (7), even as other sulfurous components reduce symptoms  
79 (8). Diet can be beneficial or detrimental to gut inflammation (9), but IBD patients choose to avoid  
80 all fiber based on a lost nuance that only some fiber sources and situations may induce negative

81 side effects, e.g., (10). Thus, a better understanding of the interaction of diet, microorganisms, and  
82 disease is needed before dietary recommendations can be made.

83 Diets which are high in cruciferous vegetables such as broccoli have been associated with  
84 reduced inflammation and cancer risk (11–15) due to a group of specific plant secondary  
85 compounds, glucosinolates, which are used for defense against insect herbivory. Glucosinolates  
86 are very high in broccoli and can be converted into bioactive metabolites (16–18) such as sulfur-  
87 containing isothiocyanates, by the action of myrosinase, an enzyme present in these vegetables. In  
88 humans, isothiocyanates have been identified as bioactive candidates for reducing gut  
89 inflammation (19–21). Specifically, sulforaphane (SFN), a well-studied isothiocyanate (22), has  
90 been shown to inhibit the action of Nuclear Factor – Kappa B (NF- $\kappa$ B) and Signal Transducer and  
91 Activator Of Transcription 3 (STAT3) which are responsible for upregulation of inflammatory  
92 cytokines interleukins-6, -8, -12, -21, and -23 (19, 23–26). However, raw broccoli and broccoli  
93 sprouts contain small amounts of this anti-inflammatory, as broccoli-sourced enzymes  
94 preferentially metabolize the precursor of sulforaphane, glucoraphanin (GLR), to an inactive  
95 byproduct instead (22). Cooking the sprouts can alter the enzymatic activity of broccoli enzymes  
96 to prevent the creation of an inactive byproduct, leaving glucosinolates intact.

97 Mammals do not produce the enzymes for converting glucosinolates to isothiocyanates;  
98 however, gut bacteria with  $\beta$ -thioglucosidase activity can convert GLR to bioactive SFN in the  
99 mammalian GI tract (27–29). In human participants who were pretreated with oral antibiotics and  
100 bowel cleansing, urinary isothiocyanates excretion after consumption of cooked broccoli  
101 decreased significantly (17), supporting a role for gut microbiota. Several microorganisms isolated  
102 from the mammalian gut appear to have myrosinase-like enzymes that cleave the glycoside moiety  
103 from glucosinolates precursors, and there is evidence for GLR hydrolysis to SFN by colonic and

104 cecal bacteria, *ex vivo* and *in vivo* in mono-colonized animal models (27, 30, 31). The bacterial  
105 populations that are capable of metabolizing glucosinolates precursors are not fully known, but  
106 *Lactobacillus*, *Bifidobacteria*, and *Bacteroides* strains have been implicated (20, 31, 32).

107 The taxonomic and functional structure of microbial communities along the  
108 gastrointestinal tract are highly dependent on the diet, health status, age, and microbial encounters  
109 of the host (33–35). Specific organs and sites within organs foster different environmental  
110 conditions that can create spatial niches for microbial taxa, an ecological pattern known as  
111 biogeography (36–38). For example, pH changes dramatically along the gastrointestinal tract and  
112 is linked to microbial diversity and density. IBD patients often have a less acidic gastrointestinal  
113 tract (39) due to altered diet or treatments, and this may result in alterations to gut biogeography  
114 (40), especially in mucosal-associated bacterial fractions (41–43). Mouse studies suggest  
115 biotransformation of GLR to SFN occurs in the colon (31, 44, 45), and we confirmed the majority  
116 of SFN accumulation to occur in the colon with greater resolution using multiple locations along  
117 the GI tract in our recently published study (18). Altering the structure and function of bacterial  
118 communities could alter if and where sulforaphane is created, which would improve or lessen the  
119 impact of having a locally produced anti-inflammatory on the destructive effects of colitis.

120 The dextran sodium sulfate (DSS) mouse model is widely used to reflect human Ulcerative  
121 Colitis (UC) in many ways (46, 47), and has been used for studying diet-sourced anti-  
122 inflammatories for the prevention of IBD in animals (46, 48). Administration of DSS in drinking  
123 water modifies the expression of tight junction proteins in intestinal epithelial cells, leading to a  
124 leaky epithelial barrier (49). This is followed by goblet cell depletion, erosion, ulceration, and  
125 infiltration of neutrophils into the lamina propria and submucosa (50), triggering the innate  
126 immune response (51, 52).

127 There are significant knowledge gaps regarding the biogeography of the participating  
128 microbiota and how this may impact glucosinolate metabolism and health benefits to the host; and  
129 meanwhile, how the populations of microbiota are impacted by these bioactives remains unclear.  
130 To address these, we assessed the impact of steamed broccoli sprouts on the biogeographic pattern  
131 of gut microbiota and disease outcome in a mouse model of chronic, relapsing colitis. We fed  
132 specific pathogen free (SPF) C57BL/6 mice either a control diet or a 10% steamed broccoli sprout  
133 diet, starting at 6 weeks of age and continuing for another 40 days. The fresh broccoli sprouts were  
134 steamed to inactivate plant enzymes, and thus the metabolism of glucosinolates to isothiocyanates  
135 would rely on the gut microbiota. A three-cycle regimen of DSS in drinking water was given to  
136 stimulate chronic colitis in the mice, which is a well-established method (48, 53). We analyzed the  
137 bacterial communities from the luminal-associated (i.e., digesta contents) and mucosal-associated  
138 (i.e., scrapings) fractions in the jejunum, cecum, and colon using 16S rRNA gene sequencing, and  
139 compared this to metrics of disease activity including weight gain/stagnation, fecal characteristics,  
140 and lipocalin as a surrogate marker for inflammation in IBD (Figure 1).

141

142

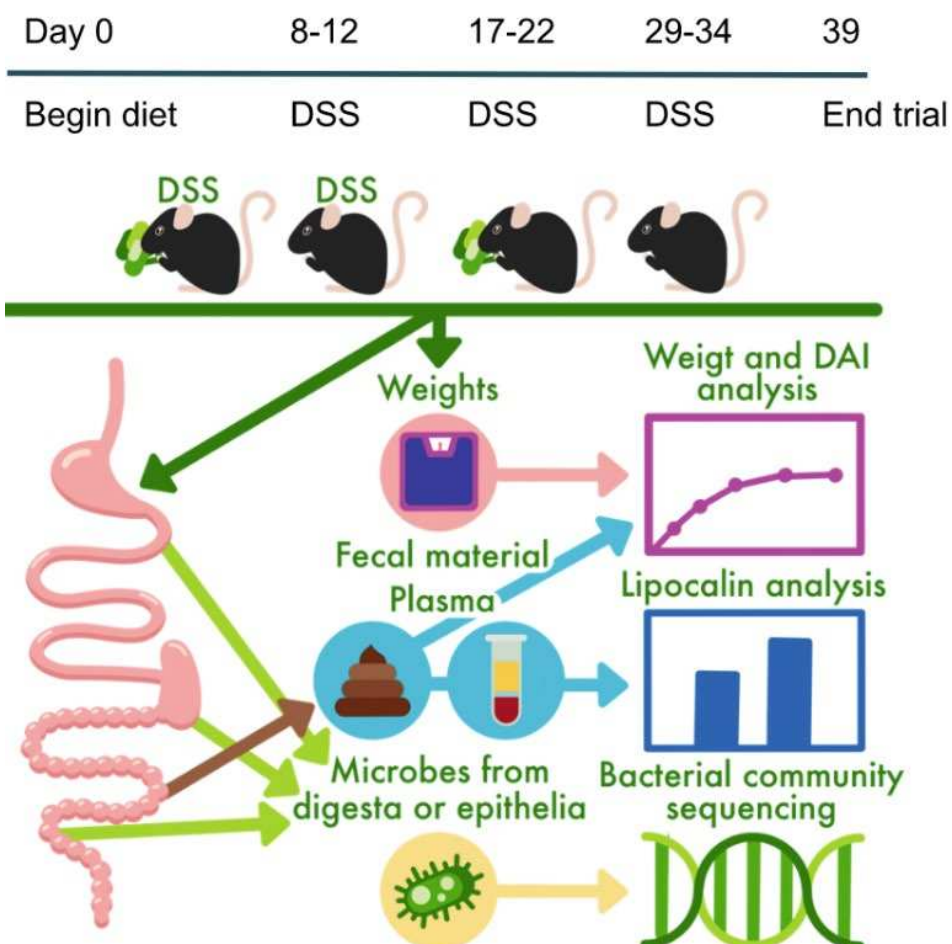
## 143 **Results**

### 144 **Broccoli sprouts alleviated disease characteristics of DSS-induced colitis**

145 Mice were divided into four groups: control diet (Control), control diet with 2.5% DSS in  
146 drinking water (Control+DSS), 10% (w/w) steamed broccoli sprout diet (Broccoli, with the control  
147 diet as the base), and 10% broccoli sprout diet with 2.5% DSS in drinking water (Broccoli+DSS)  
148 (Figure 1). The DSS regimen was designed to induce chronic, relapsing colitis (54). The 6-week-

149 old mice were acclimatized for 1 week. Treatment began in two phases: broccoli mice began their  
150 treatment at 7 weeks old (Day 0), and the first DSS cycle began at 8 weeks old (Day 8).

151



152  
153

154 **Figure 1. Experimental design schematic for a chronic model of colitis induced by dextran**  
155 **sodium sulfate (DSS) in 40 male mice (C57BL/6) beginning at 6-weeks of age.**

156

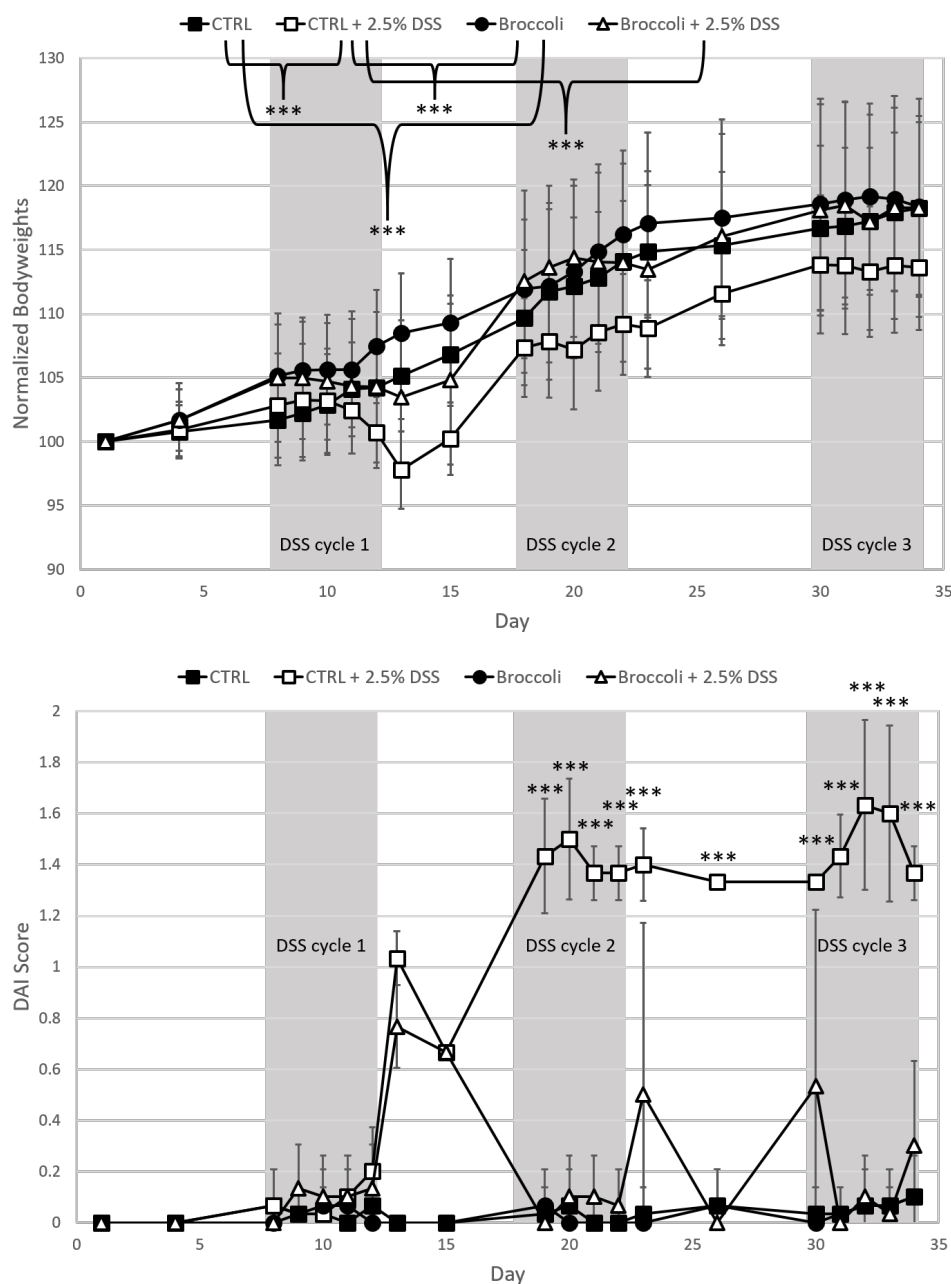
157 All mice gained weight over the study, as they are in a growth phase at this age (55). Mice  
158 receiving the steamed broccoli sprout diet and DSS (Broccoli+DSS) gained significantly more  
159 body weight over the trial than mice given the control diet and DSS (Control+DSS) (Figure 2a;  
160 ANOVA,  $p < 0.03$ ). There was no statistical difference observed in body weight among the three  
161 groups, Broccoli+DSS, Broccoli, and Control (ANOVA,  $p > 0.05$ ). Control and Broccoli mice

162 occasionally exhibited slight weight loss as compared to body weight two days prior (Figure 2a),  
163 but these appeared to be random incidents which may be attributable to mice behavior and social  
164 dynamics. At the end of the first round of DSS treatment, Broccoli+DSS mice exhibited some  
165 weight loss and Control+DSS mice exhibited substantial weight loss (Figure 2a), but the second  
166 and third round of DSS only caused weight stagnation.

167 Mice in the Control+DSS group demonstrated elevated Disease Activity Index (DAI)  
168 scores as calculated by weight loss intensity score, fecal blood, and fecal consistency. Elevated  
169 DAI scores began at day 8 and lasted until day 34 (Figure 2b), and were significant on specific  
170 dates as compared to the mice in the Control group (Figure 2b, ANOVA,  $p < 0.05$ , comparisons  
171 by day, adjusted with TukeyHSD for multiple comparisons), as well as integrated over time  
172 (generalized additive model (GAM),  $F = 308.32$ ,  $p < 2e-16$ ).

173 Mice in the Broccoli+DSS group exhibited slightly elevated DAI scores during periods of  
174 DSS treatment, which returned to nearly 0 during rest periods, and which were lower as compared  
175 to Control+DSS mice (Figure 2b). Broccoli+DSS DAI scores were significantly elevated on  
176 specific dates (Figure 2b, ANOVA,  $p < 0.05$ , comparisons by treatment, adjusted with TukeyHSD  
177 for multiple comparisons), as well as integrated over time (GAM,  $F = 17.47$ ,  $p < 2e-16$ ). After the  
178 first round of DSS treatment, Broccoli+DSS and Control+DSS mice had similar elevated DAI  
179 scores (Figure 2b, ANOVA,  $p > 0.05$ ). The diet control groups which were not treated with DSS,  
180 Control and Broccoli, did not have significantly different DAI scores from each other at any  
181 specific date (ANOVA,  $p > 0.05$ ) or over time (GAM,  $p > 0.05$ ). There was a lot of variability in  
182 the amount of fecal lipocalin between mice in treatment groups (Figure 3A), resulting in a lack of  
183 statistical significance between mice receiving DSS on the control diet and the steamed broccoli  
184 sprout diet except for day 19 on which steamed group had significantly (ANOVA,  $p < 0.05$ ) higher

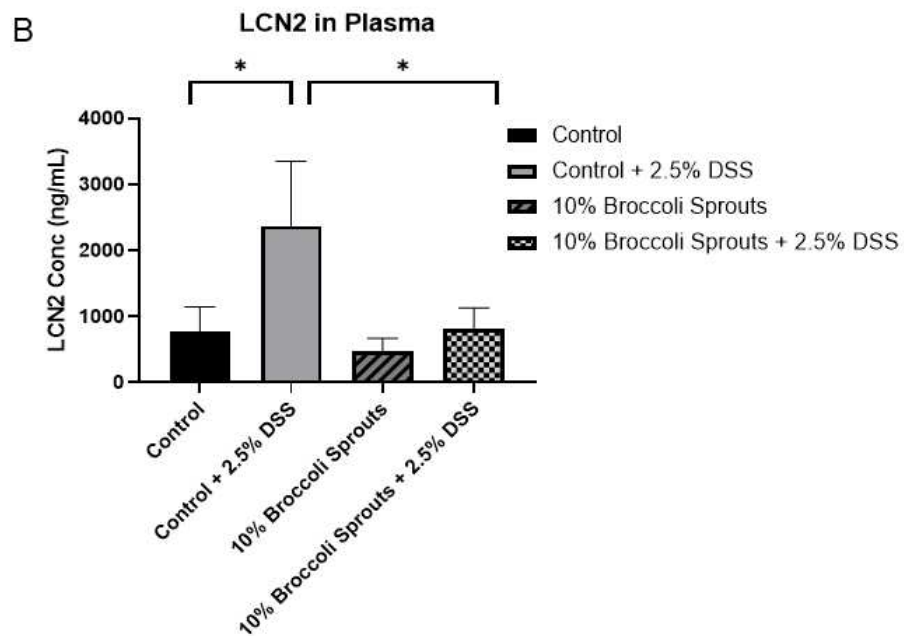
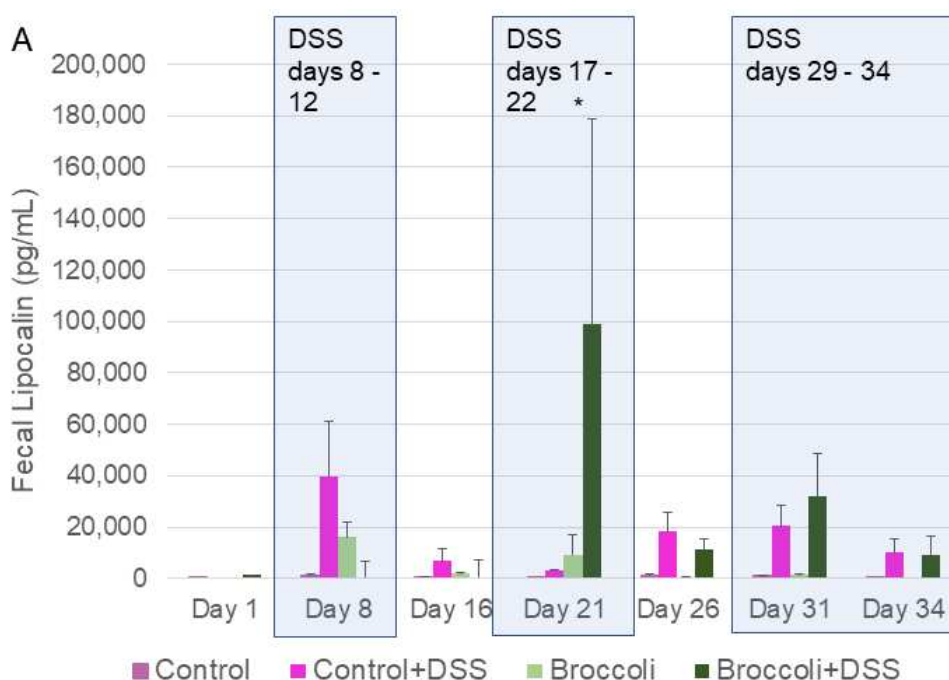
185 lipocalin levels. Analysis of plasma samples showed DSS increased lipocalin levels in the plasma  
186 (Figure 3B). Feeding the mice with a 10% broccoli sprouts diet reduced the lipocalin levels in the  
187 group of mice treated with DSS comparable to the control group without DSS treatment (ANOVA,  
188  $p < 0.05$ ).



189  
190 **Figure 2. Metrics of disease status in a DSS-Induced model of chronic colitis, including (A)**  
191 **mouse body weights and (B) Disease Activity Index, by day of experiment.** Body weights and

192 time scale were normalized to the day mice began the broccoli sprout diet. DAI scores are  
193 calculated by weight loss intensity score, fecal blood, and fecal consistency. Treatment  
194 comparisons at each day compared by ANOVA, and significance is designated as 0 - 0.001 \*\*\*.  
195 Four treatment groups were used in a 34-day chronic, relapsing model of colitis: control diet,  
196 control diet with DSS added to drinking water, control diet adjusted with 10% by weight steamed  
197 broccoli sprouts, and 10% broccoli sprout diet with DSS added to drinking water.

198



199

200 **Figure 3 Lipocalin in (A) feces at multiple timepoints and (B) serum on the last day of the**  
201 **trial from mice in a DSS-Induced model of chronic colitis.** Significance was determined as  $p <$   
202  $0.05$ , ANOVA.

203

204 Of the mice which had an elevated DAI score, some mice were positive for fecal blood,  
205 which can select for certain bacteria in the gut. In a subset of samples of mice which had an  
206 elevated DAI and were positive for fecal occult blood, there were different gut bacteria which were  
207 identified as important community features depending on whether they received the Control+DSS  
208 or the Broccoli+DSS diets (Figure 4,  $p < 0.05$ ). In Broccoli+DSS mice with positive fecal blood  
209 scores, these important taxa included a bacterial sequence variant (SV) identified in the  
210 Muribaculaceae family, and one in the *Clostridium* sensu stricto clade (Figure 4). For  
211 Control+DSS mice with a positive fecal blood score, this included different SVs identified in the  
212 *Clostridium* sensu stricto clade, *Cutibacterium*, and others (Figure 4).



213

214 **Figure 4. Gut bacterial taxa identified from mice receiving DSS which were associated with**  
215 **having a positive fecal occult blood score on the last day of the experiment, by treatment.**  
216 Data were subset to mice with a positive score on the last day of the experiment, when the gut  
217 samples were collected. Important features (SVs) were identified through permutational random  
218 forest analysis, and only the features important to this group (>50 reads) are listed out of 143  
219 significant ( $p < 0.05$ ) features across all treatments. Model accuracy was 89.7%. Bacterial  
220 sequence variants (SV) are identified as the lowest level of taxonomic identity possible, with “NA”  
221 indicating which could not be identified to species, and the number indicating which specific SV  
222 it was. Four treatment groups were used in a 34-day chronic, relapsing model of colitis, those  
223 included here are a control diet with DSS added to drinking water, and 10% broccoli sprout diet  
224 with DSS added to drinking water.

225

226 **Broccoli sprouts increased bacterial richness even during colitis**

227 Across all treatments and all mouse gastrointestinal samples, bacteria were primarily  
228 identified as belonging to the phyla *Bacillota* (formerly *Firmicutes*), *Bacteroidota* (formerly  
229 *Bacteroidetes*), *Pseudomonadota* (formerly *Proteobacteria*), *Actinomycetota* (formerly  
230 *Actinobacteria*) which was higher in Control+DSS mice, and *Verrucomicrobiota* (formerly  
231 *Verrucomicrobia*) which was higher in mice consuming broccoli sprouts (Figure S1).

232 Compared to the Control mice (receiving the control diet without DSS treatment), all other  
233 treatment groups had more bacterial taxa present (measured as observed richness) in all locations  
234 examined, with the exception of a loss of richness in the digesta/contents of the cecum and colon  
235 in Control+DSS mice (Figure 5, Table 1, linear regression). Broccoli and Broccoli+DSS mice had  
236 the highest bacterial richness in all gut locations, particularly in the colon contents and scraping,  
237 but even the Control+DSS mice maintained high bacterial richness.



238

239 **Figure 5. Observed bacterial richness along the intestinal of mice on control diets with or**  
240 **without broccoli sprouts, and with or without DSS-induced chronic repeating colitis.**  
241 Richness is calculated as the number of different bacterial sequence variants (SVs). Statistically  
242 significant comparisons are provided in Table 1. Four treatment groups were used in a 34-day  
243 chronic, relapsing model of colitis: control diet, control diet with DSS added to drinking water,  
244 control diet adjusted with 10% by weight steamed broccoli sprouts, and 10% broccoli sprout diet  
245 with DSS added to drinking water.

246

247 **Table 1. Statistical comparison of observed richness along the intestinal of mice on control**  
248 **diets with or without broccoli sprouts, and with or without DSS-induced chronic repeating**  
249 **colitis.** Comparisons were made using linear regression models comparing treatment, in subsets of  
250 the data by anatomical location. Only significant comparisons ( $p < 0.05$ ) are listed. Bacterial  
251 richness is visualized in Figure 5.

Treatment compared to control diet only group	Change in bacterial richness (SVs) $\pm$ Standard Error (rounded)	T-value	P-value
---	---	---------	---------

<b>Jejunum contents</b>			
Control + 2.5% DSS	40 ± 11	3.790	0.000608 ***
10% Broccoli sprouts	23 ± 10	2.766	0.009207 **
10% Broccoli sprouts + 2.5% DSS	64 ± 10	6.141	5.05e-07 ***
<b>Jejunum scraping</b>			
Control + 2.5% DSS	52 ± 17	3.04	0.00434 **
10% Broccoli sprouts	98 ± 16	6.230	1.16e-06 ***
10% Broccoli sprouts + 2.5% DSS	100 ± 15	6.708	3.35e-07 ***
<b>Cecum contents</b>			
Control + 2.5% DSS	-13 ± 15	-0.821	0.418
10% Broccoli sprouts	68 ± 13	5.120	1.54e-05 ***
10% Broccoli sprouts + 2.5% DSS	70 ± 13	5.225	1.54e-05 ***
<b>Colon contents</b>			
Control + 2.5% DSS	-12 ± 9	-1.316	0.197
10% Broccoli sprouts	43 ± 9	4.525	6.67e-05 ***
10% Broccoli sprouts + 2.5% DSS	90 ± 10	9.172	7.74e-11 ***
<b>Colon scraping</b>			
Control + 2.5% DSS	14 ± 12	1.225	0.129
10% Broccoli sprouts	60 ± 12	5.220	1.78e-05 ***

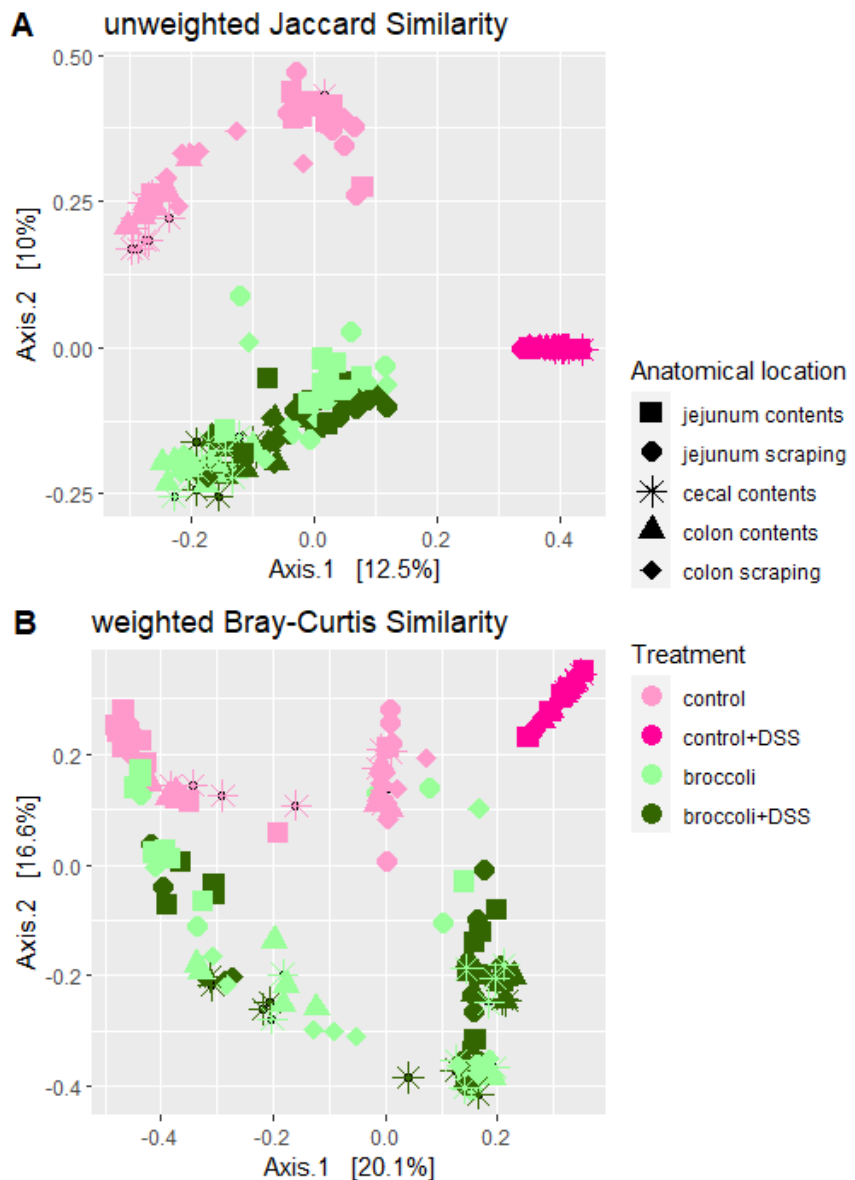
10% Broccoli sprouts + 2.5% DSS	89 ± 12	7.749	2.81e-08 ***
---------------------------------	---------	-------	--------------

252

253 **Broccoli sprouts protected against DSS-induced changes to bacterial communities**

254 Treatment was the most significant driver of bacterial community similarity in the  
255 gastrointestinal tract of mice (Figure 6a,b), when considering which bacterial taxa were  
256 present/absent (unweighted Jaccard Similarity, permANOVA:  $F = 16.90$ ,  $p < 0.001$ ) or when  
257 considering presence as well as abundance (weighted Bray-Curtis Similarity, permANOVA:  $F =$   
258  $29.97$   $p < 0.001$ ). Mice fed a control diet clustered away from other treatments, as did mice on a  
259 control diet with DSS-induced colitis, while mice on a broccoli sprout diet overlapped with mice  
260 eating sprouts along with DSS-induced colitis (Figure 6a, b).

261 Using both metrics for calculating similarity, we evaluated the distance from centroids to  
262 samples by treatment group (beta dispersion), as an indication of the strength of each treatment in  
263 selecting bacterial communities. The Broccoli and Broccoli+DSS samples had the same amount  
264 of dispersal between samples and the centroid for that treatment (beta dispersion,  $p > 0.05$  for both  
265 comparisons, adjusted with Tukey's Honestly Significant Difference correction for multiple  
266 comparisons), while Control and Control+DSS groups had very different amounts of dispersal  
267 between the samples and the centroids respective to those treatments (beta dispersion,  $p < 0.05$  for  
268 both comparisons, adjusted with Tukey's HSD).



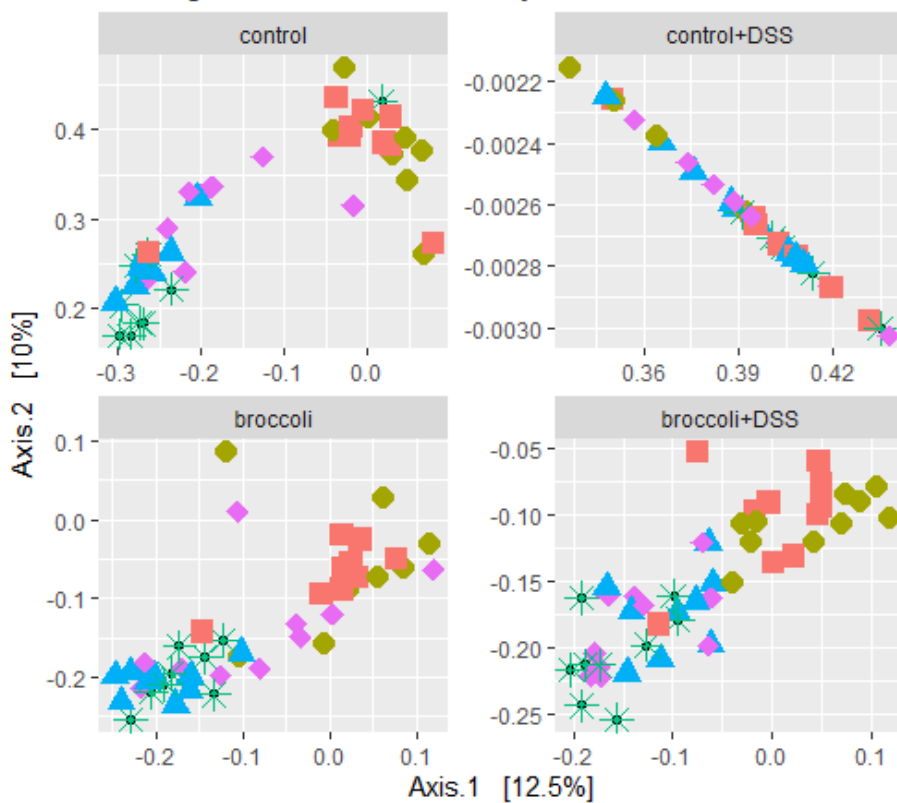
269

270 **Figure 6. Principal coordinate analysis of bacterial community similarity along the intestines**  
271 **of mice on control diets with or without broccoli sprouts, and with or without DSS-induced**  
272 **chronic repeating colitis.** Panel A was calculated with unweighted Jaccard Similarity to visualize  
273 differences in the taxonomic structure, and panel B with weighted Bray-Curtis to visualize  
274 structure and abundance. Four treatment groups were used in a 34-day chronic, relapsing model of  
275 colitis: control diet, control diet with DSS added to drinking water, control diet adjusted with 10%  
276 by weight steamed broccoli sprouts, and 10% broccoli sprout diet with DSS added to drinking  
277 water.

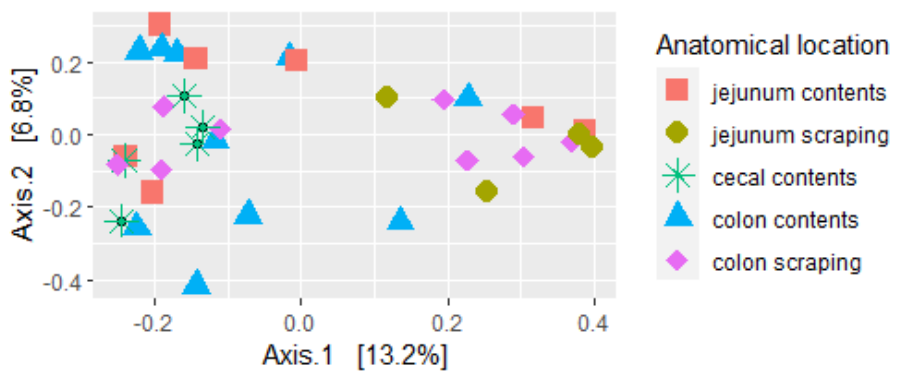
278

279 Within the clusters of bacterial communities for each treatment, there was a secondary  
280 clustering effect of anatomical location, i.e., biogeography (Figure 7; permANOVA, uJS:  $F = 3.42$ ,  
281  $p < 0.001$ ; wBC:  $F = 4.36$ ,  $p < 0.001$ ). This is easily visualized in Control, Broccoli, and  
282 Broccoli+DSS groups (Figure 6a, b), but was not observed in Control+DSS when compared with  
283 the other samples. When comparing all diet treatments, the variation between the Control+DSS  
284 group and the other treatments is so large that it obscures trends within the group (Figure 7a). Thus,  
285 we subset the Control+DSS samples (Figure 7b), and observed that the DSS alone diminishes the  
286 effect of biogeography such that there is no statistical difference (permANOVA,  $p > 0.05$ ), except  
287 marginally between jejunum scraping vs. cecum ( $p = 0.04$ ), between anatomical locations when  
288 considering the bacterial community structure (unweighted Jaccard Similarity; Figure 7b) or  
289 structure and abundance (weighted Bray-Curtis, data not shown).

**A unweighted Jaccard Similarity**



**B unweighted Jaccard Similarity on Control + DSS only**



290

291 **Figure 7. Principal coordinate analysis of bacterial communities from locations along the**  
292 **intestines of mice, across all treatments (A) and in DSS-induced colitis alone (B).** Bacterial  
293 communities in the jejunum, cecum, and colon were statistically different (permANOVA,  $p < 0.05$ )  
294 from each other in the treatment groups (A) Control, Broccoli, and Broccoli+DSS, were not  
295 statistically different from each other after multiple bouts of colitis in the (B) Control+DSS group.  
296

297

298 When identifying significant taxa which defined the samples in different treatments, there  
299 were 188 significant ( $p < 0.05$ ) features across all treatments with a permutational random forest  
300 model accuracy of 98%. The Control mice contained a high abundance of mouse commensals,  
301 such as *Dubosiella* spp. and strains from the Muribaculaceae and Lachnospiraceae families (Figure  
302 S2). The Control+DSS mice contained much lower abundance of those known mouse commensal  
303 taxa and higher abundance of the *Clostridium sensu stricto* clade (Figure S3). The Broccoli sprout  
304 group was high in *Dubosiella* spp., *Parasutterella exrementihominis*, and *Bacteroides* spp.  
305 (Figure S4). The Broccoli+DSS group had many of the same important taxa as the group  
306 consuming Broccoli sprouts without colitis (Figure S5), implying a strong selective pressure of the  
307 broccoli sprouts on the bacterial community structure such that many SVs were found in high  
308 abundance across at least 70% of the samples in those mice (Figure S6). There were no bacterial  
309 SVs which were shared across at least 70% of samples in the Broccoli+DSS and the Control+DSS  
310 group, indicating there was not a specific community which was enriched or associated with the  
311 DSS.

312

313 **Genera with putative GLR metabolism capacity present with broccoli sprout diet even**  
314 **during colitis**

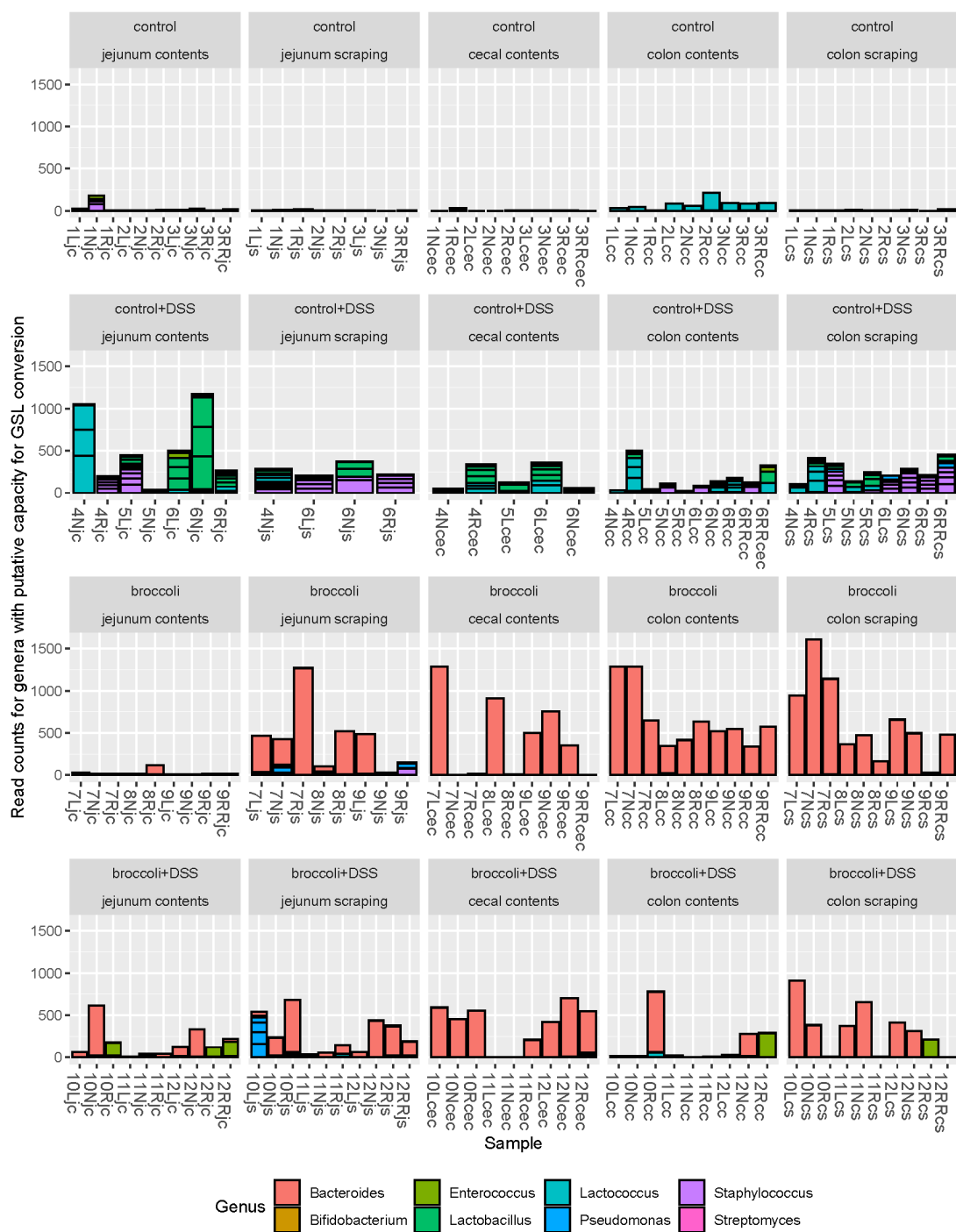
315 There are several bacterial taxa which are known or reputed to express myrosinase-like  
316 enzymatic activity and transform glucoraphanin into sulforaphane, and we selected taxa from  
317 previous literature to examine in greater detail (31, 56, 57). There were 309 bacterial SVs identified  
318 to the genera *Bifidobacterium*, *Bacteroides*, *Enterococcus*, *Lactobacillus*, *Lactococcus*,  
319 *Pseudomonas*, *Staphylococcus*, and *Streptomyces*. We found no *Faecalibacterium*, *Bacillus*,  
320 *Listeria*, *Pediococcus*, *Aerobacter*, *Citrobacter*, *Enterobacter*, *Escherichia*, *Salmonella*,

321 *Paracolobactrum*, or *Proteus* in our samples (Figure 8). Only a few of these were found in Control  
322 mice, with some of these genera found in the jejunum of Control+DSS mice (Figure 8), although  
323 without species-level resolution it cannot be determined if these are beneficial strains.

324 Importantly, most of these reads belonged to *Bacteroides* (1,394,934 frequency across all  
325 samples compared to a total frequency of 6,791 for all other sequences) and were found along the  
326 gastrointestinal tract of mice consuming the broccoli sprout diet, with or without DSS (Figure 8),  
327 suggesting improved GLR metabolism capacity upon the exposure to broccoli sprout diet.  
328 However, for the broccoli and DSS treatment, only the cecum contents and colon scrapings  
329 retained a significant proportion of *Bacteroides*. The *Bacteroides* content of the colon contents  
330 appears to have been adversely affected by the addition of DSS to the broccoli diet.

331

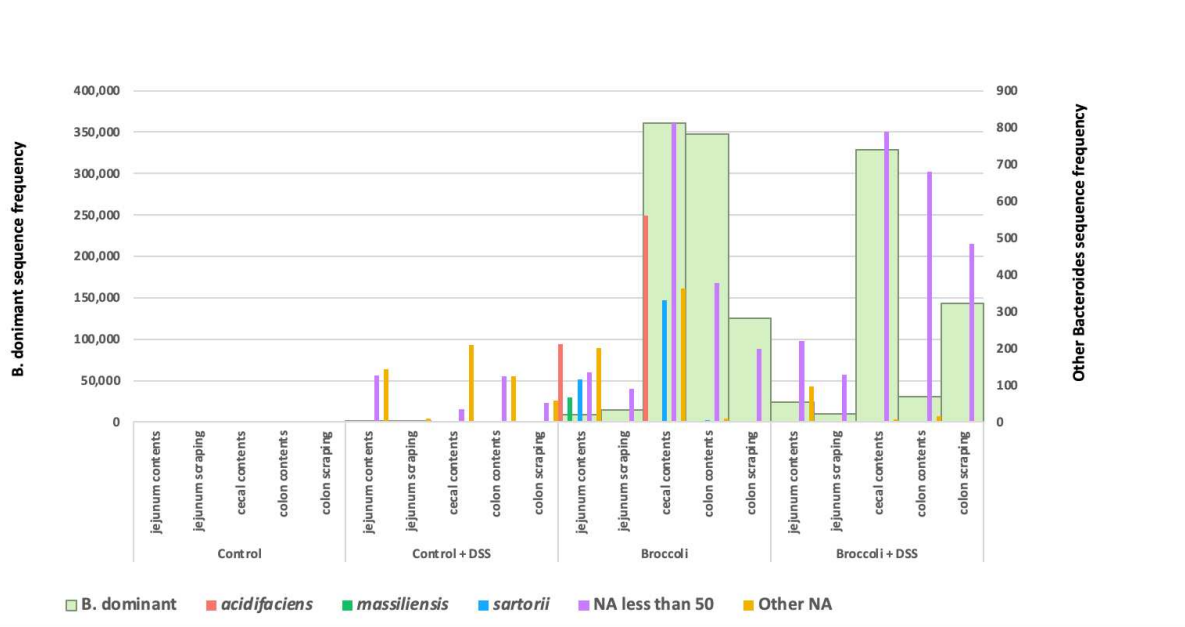
332



333  
334 **Figure 8. Bacterial sequence variants (SVs) belonging to the genera which have putative**  
335 **capacity to convert glucoraphanin to sulforaphane.** Strains of bacteria in these genera have  
336 been demonstrated to perform myrosinase-like activity in the digestive tract, as reviewed in (56).  
337 Four treatment groups were used in a 34-day chronic, relapsing model of colitis: control diet,  
338 control diet with DSS added to drinking water, control diet adjusted with 10% by weight steamed  
339 broccoli sprouts, and 10% broccoli sprout diet with DSS added to drinking water.

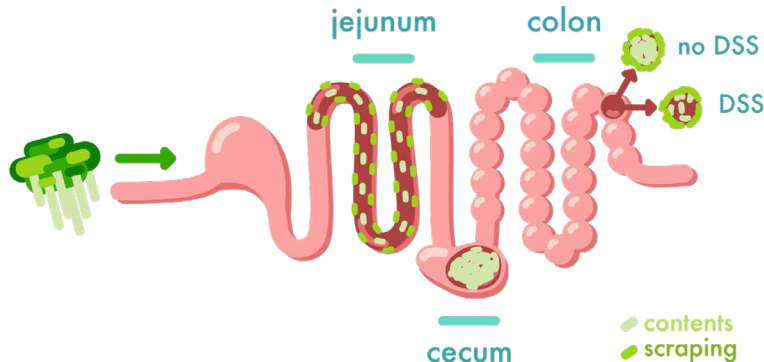
340  
341

342 Several *Bacteroides* species were identified (*acidifaciens*, *massiliensis*, *sartorii*), but the  
343 dominant sequence variant was not identified to species-level by the Silva Database taxonomy  
344 assignment (Figure 9, 10). This unidentified *Bacteroides* dominant SV (*B.*-dominant) may be  
345 associated with multiple species using the NCBI Database (BLASTN): *Bacteroides*  
346 *thetaiotaomicron* (*B. theta*), *Bacteroides faecis* and *Bacteroides zhangwenhongii* (all with 100%  
347 Query Cover and Percent Identity). *B. theta* has been linked to myrosinase-like enzyme activity  
348 and a broccoli diet, but *Bacteroides faecis* and *Bacteroides zhangwenhongii* have not.



349  
350 **Figure 9. Bacteroides species by diet treatment and anatomical location in the**  
351 **gastrointestinal tract of mice.** The Silva Database identified *Bacteroides* species *acidifaciens*,  
352 *massiliensis*, and *sartorii*. Of the BLASTN identified species for *B.*-dominant SVs, *B.*  
353 *thetaiotaomicron* was the only species only found in broccoli-sprout-fed mice.

354



355

356 **Figure 10. Biogeography of the dominant *Bacillus* SV, which was found exclusively in**  
357 **broccoli-sprout-fed mice.** *B.*-dominant was present in the jejunum contents and scrapings and  
358 abundant in the cecum contents, colon contents, and colon scrapings. DSS reduced *B.*-dominant  
359 colon content density.

360

361

362

### 363 **Discussion**

#### 364 **Broccoli sprouts protected mice against DSS-induced colitis**

365 The anti-inflammatory effects of broccoli and broccoli sprout bioactives, in particular  
366 sulforaphane (SFN), have been well-established in various cell, animal, and human trials of IBD  
367 (22). However, studies have not elucidated the role of the gut microbiota and the effect of  
368 biogeography in metabolizing the glucoraphanin (GLR) precursor to SFN, and the subsequent  
369 prevention and alleviation of inflammation in the gut. The present study sought to address these  
370 investigatory gaps by using a DSS-induced mouse model of chronic, relapsing colitis and  
371 comparing treatment group performance across multiple measures, including bacterial richness  
372 and abundance across treatment groups and anatomical locations, body weight, disease activity,  
373 and lipocalin analysis. We fed a 10% steamed broccoli sprout diet to SPF C57BL/6 mice beginning

374 at 6 weeks old and throughout a three-cycle regimen of DSS. Here, we showed that a diet featuring  
375 10% steamed broccoli sprouts reduced the Disease Activity Index and prevented DSS-induced  
376 shift in bacterial community structures along the intestines. This included preventing a shift in the  
377 microbial community caused by fecal blood, which can increase the abundance of pathobionts and  
378 reduce commensals (58, 59).

379 We began broccoli sprout feeding prior to introducing DSS, in part to acclimate mice to  
380 the diet, but primarily to investigate the use of broccoli sprouts as a prevention strategy before the  
381 initiation of colitis, as its usefulness in alleviating symptoms during active disease states has been  
382 previously demonstrated (18). We chose 10% to demonstrate proof of concept and used male mice  
383 as they are known to suffer more histopathological damage from DSS-induced colitis (60–62).  
384 Regular access to fiber is critical to recruiting and retaining beneficial microbiota in the gut (63),  
385 and regular exposure to glucosinolates is needed to stimulate gut microbial conversion (30). In  
386 people sporadically consuming broccoli or broccoli sprouts, or consuming over short periods of  
387 time, cooking preparation and the activity/inactivity of plant myrosinase were often the  
388 determining factors in how much SFN was produced, if any, as reviewed in (30). However,  
389 providing SFN directly in the diet is not feasible because it is unstable (64), and also would  
390 preclude other benefits, and the enjoyability, of consuming a phenol and fiber-rich food.

391 We acknowledge that a major limitation in this study was only using male mice, as it is  
392 known that hormones mediate both the gut microbiome and the type and intensity of DSS-induced  
393 colitis. Thus, any future research on the application of this diet in people will require diversity in  
394 the gender of participants.

395

396 **Bacterial communities are highly responsive to DSS and broccoli sprouts**

397 Mice fed broccoli sprout diets showed increased bacterial richness with and without DSS  
398 compared to mice fed a control diet. We previously showed that the concentration of SFN is  
399 highest in the colon after feeding C57BL/6 mice steamed broccoli sprout diets with reduced  
400 myrosinase concentrations, suggesting that primary hydrolysis of SFN to GLR by microbial  
401 communities occurs in the colon [32]. The current study found effects on microbial richness from  
402 the broccoli sprout diet manifested most strongly in the colon, supporting our previous findings.  
403 Given the location-specific dynamics of gut anatomy and physiology, digestion and the availability  
404 of different nutrients, and microbial communities, a smaller change in jejunum tissues could  
405 indicate that the biochemical effects of the diet are not available to the host until it reaches the  
406 colon.

407 When identifying significant taxa which defined the samples in different treatments, the  
408 Control mice contained a high abundance of known mouse commensal taxa, including *Dubosiella*  
409 spp. and strains from the Muribaculaceae and Lachnospiraceae families. The Control+DSS mice  
410 contained much lower abundance of known mouse commensal taxa and higher abundance of the  
411 *Clostridium sensu stricto* clade (65), which contains known pathogens such as *Clostridium*  
412 *perfringens* (66), and well-known butyrate-producing symbionts, such as *Clostridium butyricum*  
413 (67).

414 The Broccoli sprout group was also high in commensal taxa such as *Dubosiella* spp., and  
415 had enrichment of *Bacteroides* spp., a genus known to contain glucosinolate-metabolizing bacteria  
416 and modified by cruciferous vegetable consumption (68). The broccoli sprout diet also enriched  
417 for *Parasutterella excrementihominis*, which is commonly found in human murine gut  
418 communities and is associated with carbohydrate intake (69). It is possible that other breakdown

419 products of glucosinolates, such as aromatic carbohydrate compounds in broccoli sprouts (70),  
420 caused this enrichment. *P. excrementihominis* has also been associated with inflammation in the  
421 gut in observation-based studies; however in metabolic pathway-based studies it appears to be an  
422 important contributor to nitrate reduction in the gut and in reducing stress-related inflammation  
423 (71). Nitrates are low in raw broccoli and other cruciferous vegetables, but this can be increased  
424 by freezing (72). Thus, our diet preparation – which included freezing and freeze-drying steps –  
425 may have selected for nitrate-reducers.

426 Importantly, the Broccoli+DSS group had many of the same important taxa as the group  
427 consuming Broccoli sprouts without colitis, implying that the selective pressure of the broccoli  
428 sprouts on the bacterial community structure may be stronger than that of the DSS. The two  
429 treatments were so similar that many SVs were found in high abundance across at least 70% of the  
430 samples in those mice. There were no bacterial SVs shared across at least 70% of the  
431 Broccoli+DSS and the Control+DSS group, indicating there was not a specific community which  
432 was enriched or associated with the DSS.

433 The inclusion of DSS in drinking water demonstrably affects mice and gut bacterial  
434 communities, but it does not necessarily reduce bacterial richness. In part, this is because certain  
435 bacteria, like *Proteus vulgaris*, can make use of DSS (73), while other novel commensals appear  
436 to offer protective effects (74). We did not identify any bacterial SVs belonging to *Proteus*,  
437 although we found significantly higher amounts of *Bacteroides* sp. in broccoli sprout-fed mice.  
438 *Bacteroides thetaiotaomicron* has been demonstrated to metabolize glucoraphanin to sulforaphane  
439 and offer protection against colitis in mice (31). In this experiment, for the broccoli and niche  
440 microbiomes, *B.*-dominant flourished in the cecum and colon. *B.*-dominant was present under  
441 broccoli treatment (no DSS) in the jejunum contents and scrapings, but was abundant in the cecum

442 contents and the colon contents and scrapings. However, for the broccoli and DSS treatment, DSS  
443 presence in the colon contents did not provide as favorable an environment for *B.*-dominant.

444 Across multiple mouse lineages, individualized bacterial communities responded  
445 differently to the inclusion of DSS, and the presence of *Duncaniella muricolitica* and *Alistipes*  
446 *okayasuensis* were implicated in better mouse health outcomes (75). Modeling of the gut  
447 microbiome indicates that certain taxa may act as keystone species – critical to building the rest of  
448 the community and particularly in circumstances in which the microbial community has been  
449 destabilized (76). However, no singular important bacteria has been identified in meta analyses of  
450 IBD in humans (77, 78), and some studies have pointed to the switch from bacterial commensals  
451 to pathobionts as important (79).

452 There is considerable evidence that microbes provide metabolism of biologically inert  
453 glucosinolates to biologically active isothiocyanates, and several cultured bacterial strains from  
454 fermented foods and the digestive tract have been shown to perform this conversion (31, 56, 57).  
455 Additionally, a single bacterial equivalent of the plant myrosinase enzyme has not been identified,  
456 and there is the possibility that several enzymes in bacteria may work in concert to achieve  
457 metabolism of GSLs. Further, research is lacking to determine if the effect on the gut microbiome  
458 is metabolite (isothiocyanates)-mediated or precursor (glucosinolates)-mediated. The scope of  
459 research in this field should be expanded by investigating the concepts of biogeographic specificity  
460 of both bioactive production and absorption and microbial community dynamics.

461

## 462 **Biogeography reveals location-specific trends in the bacterial community**

463 It has been well-demonstrated that distinct bacterial communities exist in different  
464 locations along the gastrointestinal tract in mammals, related to the local anatomical,

465 environmental, nutritional, and host immunological conditions in different organs (36, 80, 81).  
466 Further, the effect of foods on the gut microbiome can be specific to an individual's communities  
467 (34). Given the complexity of microbial community function, as well as the spatially explicit  
468 biochemical digestion activities of the host, it follows that the location of glucoraphanin  
469 metabolism may influence how well the host can absorb SFN, whether it may be distributed  
470 systematically, and where it will be effective at preventing or treating symptoms. It has previously  
471 been demonstrated in mouse trials using 2,4,6 trinitrobenzene sulfonic acid to chemically induce  
472 colitis that the mucosal-associated bacterial population is more affected by colitis than the lumen-  
473 associated (digesta) community (43).

474 Here, we showed that DSS-induced colitis effectively erased the biogeographical  
475 specificity of communities in the mouse gastrointestinal tract (Figure 4, Table 1), with the  
476 exception of communities in jejunum scrapings remaining distinct from those in cecal contents.  
477 Given the highly specific function of the cecum in separating fibers by size and furthering  
478 microbial fermentation, it is not surprising that it would be distinct. The DSS may be a stronger  
479 selective force than anatomical location in driving bacterial communities in the gut (74). For  
480 example, its destruction of the epithelial cell surface may change the microarchitecture and alter  
481 microbial attachment in the gut (82), and DSS increases the hydrophobicity of bile acids (83),  
482 which may affect microbial survival and ability to attach to host epithelial cells, thus increasing  
483 microbial washout through the gut. Any of these could possibly explain our findings that DSS  
484 eliminated biogeographical specificity of communities in the mouse gastrointestinal tract.  
485 However, more research would be needed to determine causation.

486 Mouse studies suggest biotransformation of glucoraphanin to SFN occurs in the colon (31,  
487 44, 45), and we previously confirmed the majority of SFN accumulation takes place in the colon,

488 with greater resolution using multiple locations along the GI tract (18). Critically, the cecum had  
489 low SFN, indicating that it is not responsible for hosting bacterial biotransformation of these  
490 bioactives (18). Here, we also showed that only a few bacterial taxa were estimated to be sourced  
491 in the cecum and creating sink populations in the colon (Figure S7), and of these, none were  
492 identified to be putatively responsible for metabolism of glucoraphanin. Collectively, this confirms  
493 that this is a valid model for generalization to the human gut.

494

#### 495 **Considerations for the application of this work**

496 Access to fresh or frozen broccoli and broccoli sprouts, the cooking preparation, and the  
497 ability to regularly consume these vegetables will have implications for the feasibility and success  
498 of a dietary intervention for preventing or reducing inflammation in the gut. For example, sprouts  
499 from various plants have been implicated in food-borne illness because of their proximity to soil,  
500 and people may be wary of or discouraged from consuming raw or slightly cooked sprouts.  
501 However, more recent research has shown that sprouts can be consumed safely, especially with  
502 improvements in hygiene and agricultural regulations, as well as in food processing (84). Further,  
503 broccoli sprouts can be grown at home in windowsill seed-bed germinators without requiring soil,  
504 gardening tools, or specialized gardening knowledge, which could ease the financial burden of  
505 purchasing healthy foods (85). This may prove to be particularly important in areas without access  
506 to healthcare or affordable prescriptions, or in areas without close proximity to fresh, healthy fruits  
507 and vegetables (7, 86, 87) as this can preclude being able to make the dietary recommendations  
508 set forth by medical professionals (88). Including broccoli sprouts as 10% of the diet could be  
509 potentially too high for IBD patients to comply with, and future studies on the application of this

510 diet will require a deeper understanding of the biological, microbiological, immunological, as well  
511 as social and logistical factors involved in dietary interventions in people.

512

513

514 **Materials and Methods**

515 **Diet preparation**

516 Jonathan's Sprouts™ (Rochester, Massachusetts, USA) broccoli sprouts were purchased  
517 from a grocery store (Bangor, Maine, USA) and steamed in a double boiler for 10 minutes and  
518 immediately cooled down. They were stored in a -80°C freezer until freeze-drying (University of  
519 Maine Pilot Plant, Orono, Maine, USA). The freeze-dried broccoli sprouts were ground into a fine  
520 powder and mixed with purified AIN93G rodent base diet to a concentration of 10% by weight.  
521 Our previous work assessed the effects of different diet preparations and the percentage of broccoli  
522 sprouts, and found that 5-10% broccoli sprouts by weight reliably produces consistent anti-  
523 inflammatory results in mice (18). For this study, we chose to use 10% steamed broccoli sprouts  
524 both to assess the microbial conversion of GLR to SFN, and to ensure that the intervention would  
525 have a strong effect. Diet pellets were formed using a silicone mold to ensure consistent sizing,  
526 and allowed to dry at room temperature for up to 48 hours in a chemical safety hood to facilitate  
527 moisture evaporation, and after drying were stored in sealable plastic bags in a -20°C freezer.

528

529 **DSS colitis model**

530 Forty male, 6-week-old, specific pathogen free (SPF) C57BL/6 mice (*Mus musculus*) were  
531 purchased from the Jackson Laboratory (Bar Harbor, Maine, U.S.) and transferred to the animal  
532 facility at the University of Maine (Orono, Maine, U.S.). The animal protocol (IACUC protocol

533 A2020-01-04) was approved by the University Committee on the Use and Care of Animals, and  
534 all biosafety work was approved by the Institutional Biosafety Committee (protocol SI-092220).  
535 The mice were acclimated to the facility for 7 days (day -7 to 0), during which they received *ad*  
536 *libitum* autoclaved tap water and the AIN-93G purified rodent diet (control diet). After initial  
537 acclimation, the mice were randomly assigned to one of 4 experimental groups beginning on  
538 experimental day 0: control diet without DSS treatment (Control), 10% steamed broccoli sprout  
539 diet without DSS treatment (Broccoli), control diet with DSS treatment (Control+DSS), and 10%  
540 steamed broccoli sprout diet with DSS treatment (Broccoli+DSS). All experimental groups were  
541 on 7 days of their respective diets (control or 10% steamed broccoli sprout), after which DSS (Alfa  
542 Aesar, molecular weight ~40 kD (53)) was added to the drinking water of the DSS treatment  
543 groups to a final concentration of 2.5%. Mice were given DSS for 5 days, followed by a recovery  
544 period for 5 - 7 days. This was repeated for a total of 3 cycles to induce chronic colitis (48, 89).  
545 Mice were sacrificed and tissue collected after the third round of DSS, on day 35 of the experiment.

546 Bodyweight, fecal blood, and fecal consistency were used to calculate Disease Activity  
547 Index (DAI) scores (52). Samples were taken every 2 - 3 days throughout the trial, and daily during  
548 the DSS cycles. Body weights and DAI were analyzed using 2-way ANOVA generated with R to  
549 compare differences between treatments for each day. A generalized additive model (GAM) was  
550 used in R to compare DAI differences (R-sq.(adj) = 0.861, Deviance explained = 86.4%, GCV =  
551 0.036031) by treatment across the entire study, using Mouse ID to account for repeated measures.  
552 Lipocalin-2 concentration in the plasma and fecal samples were determined by a mouse Lipocalin-  
553 2/NGAL DuoSet ELISA kit (R & D Biosystems, USA) following the manufacturer's instructions.  
554 Lipocalin is a neutrophil protein that binds bacterial siderophores and serves as a surrogate marker  
555 for intestinal inflammation in IBD (90). The readings at wavelengths of 540 nm and 450 nm were

556 measured by a Thermo Scientific Varioskan LUX Multimode Microplate Reader. The readings at  
557 540 nm were subtracted from the readings at 450 nm to correct for the discoloration of the solution.  
558 After euthanasia, lumen-associated (digesta contents) and mucosal-associated (epithelial  
559 scrapings) microbial community samples were collected from the jejunum, cecum (contents only),  
560 and colon for DNA extraction and community sequencing as described below.

561

## 562 **Bacterial community sequencing and analysis**

563 From the DSS mice, digesta (lumen contents) and epithelial associated (tissue scrapings)  
564 microbial community samples were collected from the jejunum, cecum (contents only), and colon.  
565 All tissues containing their resident gut microbiota were gently homogenized with vortexing, then  
566 treated with propidium monoazide (PMA; BioTium) following kit protocols at a final  
567 concentration of 25  $\mu$ m. PMA covalently binds to relic/free DNA and DNA inside  
568 compromised/dead cell membranes, and prevents amplification in downstream protocols to  
569 preclude dead DNA from the sequence data (91).

570 Following PMA treatment, bulk DNA was extracted from tissue-associated bacterial  
571 communities (n = 200 samples), or no-template (water) control samples (n = 10, one for each  
572 extraction batch) using commercially available kits optimized for water and tissue-based microbial  
573 communities (Quick-DNA Fecal/Soil Kit, Zymo Research). DNA extract was roughly quantified  
574 and purity-checked with a Thermo Scientific<sup>TM</sup> NanoDrop<sup>TM</sup> OneC Microvolume UV-Vis  
575 Spectrophotometer (Thermo Scientific, Waltham, MA, U.S.). Samples underwent DNA amplicon  
576 sequencing of the 16S rRNA gene V3-V4 region, using primers 341F [174] and 806R [175] and  
577 protocols consistent with The Earth Microbiome Project [176], and sequenced on an Illumina  
578 MiSeq platform using the 2 x 300-nt V3 kit (Molecular Research Labs, Clearwater, TX, U.S.).

579 Raw sequence data (fastq files and metadata) is available from NCBI through BioProject  
580 Accession number PRJNA911821.

581 Amplicon sequence data was processed using previously curated workflows in the Ishaq  
582 Lab (R code supplied as Supplemental Material), which used the DADA2 pipeline ver. 1.26  
583 (DADA2 Pipeline Tutorial (1.4), 2016.) in the R software environment ver. 4.1.1 [177]. The  
584 dataset started with 46,581,832 paired raw reads, and based on initial quality assessment only the  
585 forward reads were processed. Trimming parameters were designated based on visual assessment  
586 of the aggregated quality scores at each base from all samples (plotQualityProfile in DADA2): the  
587 first 10 bases were trimmed, sequences were trimmed to 225 bases in length, and were discarded  
588 if they had ambiguous bases, more than two errors, or matched the PhiX version 3 positive control  
589 (Illumina; FC-110-3001). After filtering, 34,009,802 non-unique forward/read 1 sequences  
590 remained.

591 The DADA algorithm was used to estimate the error rates for the sequencing run,  
592 derePLICATE the reads, pick sequence variants (SVs) which represent ‘microbial individuals’, and  
593 remove chimeric artifacts from the sequence table. Taxonomy was assigned using the Silva  
594 taxonomic training data version 138.1 [178] down to species where possible, and reads matching  
595 chloroplasts and mitochondria taxa were removed using the dplyr package [179]. No-template  
596 control samples were used to remove contaminating sequences from the samples by extraction  
597 batch [180]. The sequence table, taxonomy, and metadata were combined for each experiment  
598 using the phyloseq package [181], which was also used for basic visualization and statistical  
599 analysis in combination with other packages. Samples from one mouse (4L, in the Control+DSS  
600 group) were dropped from further analysis as they were outliers on all visualizations and may have  
601 been contaminated during DNA extraction.

602        Normality was checked using a Shapiro-Wilkes test on alpha diversity metrics generated  
603        from rarefied data, including observed richness, evenness, and Shannon diversity. Linear models  
604        were run for comparisons of alpha diversity metrics to compare by sample type, (lme4 package  
605        [182]), in which anatomical location and diet treatment were used as fixed effects, and mouse ID  
606        used to control for repeated sampling as needed. Generalized additive models were used to assess  
607        trends in alpha diversity using time as a smoother (92). Jaccard unweighted similarity was used to  
608        calculate sample similarity based on community membership (species presence/absence),  
609        visualized with non-parametric multidimensional scaling, and tested with permutational analysis  
610        of variance (permANOVA) by using the vegan package (93). Random forest feature prediction  
611        with permutation was used to identify differentially abundant SVs based on factorial conditions  
612        (94). Plots were made using the ggplot2 (95), ggpubr (96), and phyloseq packages.

613        Source Tracker algorithms which had been modified for the R platform (97, 98) were used  
614        to identify source:sink effects based on anatomical location. This was used to determine if the  
615        cecum could be the source for population sinks in the colon, as a proxy for the model's applicability  
616        to the human gut anatomical features and microbial communities. A total of 142 SVs were  
617        identified as possibly sourced from the cecum, and 95 SVs were estimated to make up >1% of the  
618        proportion of sources (Figure S7). The putative GLR converting bacteria in the Broccoli and  
619        Broccoli+DSS mouse gut samples were not among those taxa identified as sourced in the cecum.

620  
621  
622

## Acknowledgements

623        All authors have read and approved the final manuscript. The authors thank Jess Majors,  
624        University of Maine, for her kind and detailed care of the mice during the trial, and for Ellie  
625        Pelletier for her informal review of the manuscript. This project was supported by the USDA

627 National Institute of Food and Agriculture through the Maine Agricultural & Forest Experiment  
628 Station: Hatch Project Numbers ME022102 and ME022329 (Ishaq) and ME022303 (Li); the  
629 USDA-NIFA-AFRI Foundational Program [Li and Chen; USDA/NIFA 2018-67017-27520/2018-  
630 67017-36797]; and the National Institute of Health [Li and Ishaq; NIH/NIDDK 1R15DK133826-  
631 01]. Johanna Holman was supported by ME0-22303 (Li), and Lola Holcomb was supported by US  
632 National Science Foundation One Health and the Environment (OG&E): Convergence of Social  
633 and Biological Sciences NRT program grant DGE-1922560, and through the UMaine Graduate  
634 School of Biomedical Sciences and Engineering.

635  
636

### 637 **Author Contributions**

638 Conceptualization, S.L.I., Y.L., T.Z., G.C., G.M; Methodology, S.L.I., Y.L., T.Z., G.M., P.M.,  
639 J.H.; Software, S.L.I.; Formal Analysis, J.H., S.L.I., T.H., B.H.; Investigation, J.H., L.C., J.B.;  
640 G.C., D.B.; Resources, S.L.I., Y.L., T.Z.; Data Curation, S.L.I., J.H.; Writing - Original Draft,  
641 J.H., L.C., S.L.I., Y.L.; Writing - Review and Editing; S.L.I., Y.L., T.Z., G.M., P.M., J.H., L.C.,  
642 J.B., G.C., D.B., T.H., B.H., L.H.; Visualization, J.H., S.L.I., T.H., B.H.; Supervision, J.H.,  
643 S.L.I., Y.L., T.Z.; Project Administration, S.L.I., Y.L., T.Z.; Funding Acquisition, S.L.I., Y.L.,  
644 T.Z., G.C.

645

### 646 **Figure Legends**

647 **Figure 1. Experimental design schematic for a chronic model of colitis induced by dextran  
648 sodium sulfate (DSS) in 40 male mice (C57BL/6) beginning at 6-weeks of age.**

649

650 **Figure 2. Metrics of disease status in a DSS-Induced model of chronic colitis, including (A)  
651 mouse body weights and (B) Disease Activity Index, by day of experiment.** Body weights and  
652 time scale were normalized to the day mice began the broccoli sprout diet. DAI scores are  
653 calculated by weight loss intensity score, fecal blood, and fecal consistency. Treatment  
654 comparisons at each day compared by ANOVA, and significance is designated as 0 - 0.001  
655 ‘\*\*\*’. Four treatment groups were used in a 34-day chronic, relapsing model of colitis: control  
656 diet, control diet with DSS added to drinking water, control diet adjusted with 10% by weight  
657 steamed broccoli sprouts, and 10% broccoli sprout diet with DSS added to drinking water.

658

659 **Figure 3 Lipocalin in (A) feces at multiple timepoints and (B) serum on the last day of the**  
660 **trial from mice in a DSS-Induced model of chronic colitis.** Significance was determined as p  
661 < 0.05, ANOVA.

662 **Figure 4. Gut bacterial taxa identified from mice receiving DSS which were associated with**  
663 **having a positive fecal occult blood score on the last day of the experiment, by treatment.**  
664 Data were subset to mice with a positive score on the last day of the experiment, when the gut  
665 samples were collected. Important features (SVs) were identified through permutational random  
666 forest analysis, and only the features important to this group (>50 reads) are listed out of 143  
667 significant (p < 0.05) features across all treatments. Model accuracy was 89.7%. Bacterial  
668 sequence variants (SV) are identified as the lowest level of taxonomic identity possible, with "NA"  
669 indicating which could not be identified to species, and the number indicating which specific SV  
670 it was. Four treatment groups were used in a 34-day chronic, relapsing model of colitis, those  
671 included here are a control diet with DSS added to drinking water, and 10% broccoli sprout diet  
672 with DSS added to drinking water.

673 **Figure 5. Observed bacterial richness along the intestinal of mice on control diets with or**  
674 **without broccoli sprouts, and with or without DSS-induced chronic repeating colitis.**  
675 Richness is calculated as the number of different bacterial sequence variants (SVs). Statistically  
676 significant comparisons are provided in Table 1. Four treatment groups were used in a 34-day  
677 chronic, relapsing model of colitis: control diet, control diet with DSS added to drinking water,  
678 control diet adjusted with 10% by weight steamed broccoli sprouts, and 10% broccoli sprout diet  
679 with DSS added to drinking water.

680 **Figure 6. Principal coordinate analysis of bacterial community similarity along the**  
681 **intestines of mice on control diets with or without broccoli sprouts, and with or without**  
682 **DSS-induced chronic repeating colitis.** Panel A was calculated with unweighted Jaccard  
683 Similarity to visualize differences in the taxonomic structure, and panel B with weighted Bray-  
684 Curtis to visualize structure and abundance. Four treatment groups were used in a 34-day  
685 chronic, relapsing model of colitis: control diet, control diet with DSS added to drinking water,  
686 control diet adjusted with 10% by weight steamed broccoli sprouts, and 10% broccoli sprout diet  
687 with DSS added to drinking water.

688  
689 **Figure 7. Principal coordinate analysis of bacterial communities from locations along the**  
690 **intestines of mice, across all treatments (A) and in DSS-induced colitis alone (B).** Bacterial  
691 communities in the jejunum, cecum, and colon were statistically different (permANOVA, p <  
692 0.05) from each other in the treatment groups (A) Control, Broccoli, and Broccoli+DSS, were  
693 not statistically different from each other after multiple bouts of colitis in the (B) Control+DSS  
694 group.

695  
696 **Figure 8. Bacterial sequence variants (SVs) belonging to the genera which have putative**  
697 **capacity to convert glucoraphanin to sulforaphane.** Strains of bacteria in these genera have  
698 been demonstrated to perform myrosinase-like activity in the digestive tract, as reviewed in (56).

699 Four treatment groups were used in a 34-day chronic, relapsing model of colitis: control diet,  
700 control diet with DSS added to drinking water, control diet adjusted with 10% by weight steamed  
701 broccoli sprouts, and 10% broccoli sprout diet with DSS added to drinking water.

702  
703 **Figure 9. Bacteroides species by diet treatment and anatomical location in the**  
704 **gastrointestinal tract of mice.** The Silva Database identified *Bacteroides* species *acidifaciens*,  
705 *massiliensis*, and *sartorii*. Of the BLASTN identified species for *B.*-dominant SVs, *B.*  
706 *thetaiotaomicron* was the only species only found in broccoli-sprout-fed mice.

707  
708  
709 **Figure 10. Biogeography of the dominant *Bacillus* SV, which was found exclusively in**  
710 **broccoli-sprout-fed mice.** *B.*-dominant was present in the jejunum contents and scrapings and  
711 abundant in the cecum contents, colon contents, and colon scrapings. DSS reduced *B.*-dominant  
712 colon content density.

713

714 **References**

715 1. Peery AF, Crockett SD, Murphy CC, Lund JL, Dellon ES, Williams JL, Jensen ET,  
716 Shaheen NJ, Barritt AS, Lieber SR, Kocher B, Barnes EL, Fan YC, Pate V, Galanko J,  
717 Baron TH, Sandler RS. 2019. Burden and Cost of Gastrointestinal, Liver, and Pancreatic  
718 Diseases in the United States: Update 2018. *Gastroenterology* 156:254–272.e11.

719 2. Singh S, Qian AS, Nguyen NH, Ho SKM, Luo J, Jairath V, Sandborn WJ, Ma C. 2022.  
720 Trends in U.S. Health Care Spending on Inflammatory Bowel Diseases, 1996-2016.  
721 *Inflamm Bowel Dis* 28:364–372.

722 3. Klampfer L. 2013. Cytokines, inflammation and colon cancer. *Current Cancer Drug Targets*  
723 11:451–464.

724 4. Zhang Y-Z. 2014. Inflammatory bowel disease: Pathogenesis. *World J Gastroenterol* 20:91.

725 5. Matricona J, Barnich N, Ardid D. 2010. Immunopathogenesis of inflammatory bowel  
726 disease. *Self Nonself* 1:299–309.

727 6. Rubin DC, Shaker A, Levin MS. 2012. Chronic intestinal inflammation: Inflammatory  
728 bowel disease and colitis-associated colon cancer. *Frontiers in Immunology* 3:00107.

729 7. Walker RE, Keane CR, Burke JG. 2010. Disparities and access to healthy food in the  
730 United States: A review of food deserts literature. *Health Place* 16:876–884.

731 8. Banerjee S, Ghosh S, Sinha K, Chowdhury S, Sil PC. 2019. Sulphur dioxide ameliorates  
732 colitis related pathophysiology and inflammation. *Toxicology* 412:63–78.

733 9. Lewis JD, Abreu MT. 2017. Diet as a Trigger or Therapy for Inflammatory Bowel Diseases.

734 Gastroenterology 152:398–414.e6.

735 10. Armstrong HK, Bording-Jorgensen M, Santer DM, Zhang Z, Valcheva R, Rieger AM,

736 Sung-Ho Kim J, Dijk SI, Mahmood R, Ogungbola O, Jovel J, Moreau F, Gorman H,

737 Dickner R, Jerasi J, Mander IK, Lafleur D, Cheng C, Petrova A, Jeanson T-L, Mason A,

738 Sergi CM, Levine A, Chadee K, Armstrong D, Rauscher S, Bernstein CN, Carroll MW,

739 Huynh HQ, Walter J, Madsen KL, Dieleman LA, Wine E. 2022. Unfermented  $\beta$ -fructan

740 Fibers Fuel Inflammation in Select Inflammatory Bowel Disease Patients. Gastroenterology

741 <https://doi.org/10.1053/j.gastro.2022.09.034>.

742 11. Tse G, Eslick GD. 2014. Cruciferous vegetables and risk of colorectal neoplasms: a

743 systematic review and meta-analysis. Nutr Cancer 66:128–139.

744 12. Huang L, Li B-L, He C-X, Zhao Y-J, Yang X-L, Pang B, Zhang X-H, Shan Y-J. 2018.

745 Sulforaphane inhibits human bladder cancer cell invasion by reversing epithelial-to-

746 mesenchymal transition via directly targeting microRNA-200c/ZEB1 axis. J Funct Foods

747 41:118–126.

748 13. Li Y, Wicha MS, Schwartz SJ, Sun D. 2011. Implications of cancer stem cell theory for

749 cancer chemoprevention by natural dietary compounds. J Nutr Biochem 22:799–806.

750 14. Li Y, Zhang T, Schwartz SJ, Sun D. 2011. Sulforaphane Potentiates the Efficacy of 17-

751 Allylamino 17-Demethoxygeldanamycin Against Pancreatic Cancer Through Enhanced

752 Abrogation of Hsp90 Chaperone Function. Nutrition and Cancer

753 <https://doi.org/10.1080/01635581.2011.596645>.

754 15. Li Y, Zhang T, Korkaya H, Liu S, Lee H-F, Newman B, Yu Y, Clouthier SG, Schwartz SJ,

755       Wicha MS, Sun D. 2010. Sulforaphane, a dietary component of broccoli/broccoli sprouts,  
756       inhibits breast cancer stem cells. *Clin Cancer Res* 16:2580–2590.

757       16. Angelino D, Jeffery E. 2014. Glucosinolate hydrolysis and bioavailability of resulting  
758       isothiocyanates: Focus on glucoraphanin. *J Funct Foods* 7:67–76.

759       17. Shapiro TA, Fahey JW, Wade KL, Stephenson KK, Talalay P. 1998. Human metabolism  
760       and excretion of cancer chemoprotective glucosinolates and isothiocyanates of cruciferous  
761       vegetables. *Cancer Epidemiol Biomarkers Prev* 7:1091–1100.

762       18. Zhang T, Holman J, McKinstry D, Trindade BC, Eaton KA, Mendoza-Castrejon J, Ho S,  
763       Wells E, Yuan H, Wen B, Sun D, Chen GY, Li Y. 2022. A steamed broccoli sprout diet  
764       preparation that reduces colitis via the gut microbiota. *J Nutr Biochem* 112:109215.

765       19. Fahey JW, Stephenson KK, Wade KL, Talalay P. 2013. Urease from *Helicobacter pylori* is  
766       inactivated by sulforaphane and other isothiocyanates. *Biochem Biophys Res Commun*  
767       435:1–7.

768       20. Fahey JW, Wehage SL, Holtzclaw WD, Kensler TW, Egner PA, Shapiro TA, Talalay P.  
769       2012. Protection of humans by plant glucosinolates: efficiency of conversion of  
770       glucosinolates to isothiocyanates by the gastrointestinal microflora. *Cancer Prev Res (Phila)*  
771       5:603–611.

772       21. Wei L-Y, Zhang J-K, Zheng L, Chen Y. 2022. The functional role of sulforaphane in  
773       intestinal inflammation: a review. *Food Funct* 13:514–529.

774       22. Holman J, Hurd M, Moses P, Mawe G, Zhang T, Ishaq SL, Li Y. 2023. Interplay of

775      Broccoli/Broccoli Sprout Bioactives with Gut Microbiota in Reducing Inflammation in  
776      Inflammatory Bowel Diseases. *J Nutr Biochem* 113:109238.

777      23. Sun C-C, Li S-J, Yang C-L, Xue R-L, Xi Y-Y, Wang L, Zhao Q-L, Li D-J. 2015.  
778      Sulforaphane attenuates muscle inflammation in dystrophin-deficient mdx mice via NF-E2-  
779      related factor 2 (Nrf2)-mediated inhibition of NF-κB signaling pathway. *J Biol Chem*  
780      290:17784–17795.

781      24. Petkovic M, Leal EC, Alves I, Bose C, Palade PT, Singh P, Awasthi S, Børshem E,  
782      Dalgaard LT, Singh SP, Carvalho E. 2021. Dietary supplementation with sulforaphane  
783      ameliorates skin aging through activation of the Keap1-Nrf2 pathway. *J Nutr Biochem*  
784      98:108817.

785      25. Mazarakis N, Snibson K, Licciardi PV, Karagiannis TC. 2020. The potential use of l-  
786      sulforaphane for the treatment of chronic inflammatory diseases: A review of the clinical  
787      evidence. *Clin Nutr* 39:664–675.

788      26. Zhang Y, Tan L, Li C, Wu H, Ran D, Zhang Z. 2020. Sulforaphane alter the microbiota and  
789      mitigate colitis severity on mice ulcerative colitis induced by DSS. *AMB Express* 10:119.

790      27. Liu X, Wang Y, Hoeflinger JL, Neme BP, Jeffery EH, Miller MJ. 2017. Dietary Broccoli  
791      Alters Rat Cecal Microbiota to Improve Glucoraphanin Hydrolysis to Bioactive  
792      Isothiocyanates. *Nutrients* 9.

793      28. Manichanh C, Rigottier-Gois L, Bonnaud E, Gloux K, Pelletier E, Frangeul L, Nalin R,  
794      Jarrin C, Chardon P, Marteau P, Roca J, Dore J. 2006. Reduced diversity of faecal  
795      microbiota in Crohn’s disease revealed by a metagenomic approach. *Gut* 55:205–211.

796 29. Palop ML, LLanos Palop M, Smiths JP, ten Brink B. 1995. Degradation of sinigrin by  
797 *Lactobacillus agilis* strain R16. International Journal of Food Microbiology  
798 [https://doi.org/10.1016/0168-1605\(95\)00123-2](https://doi.org/10.1016/0168-1605(95)00123-2).

799 30. Angelino D, Dosz EB, Sun J, Hoeflinger JL, Van Tassell ML, Chen P, Harnly JM, Miller  
800 MJ, Jeffery EH. 2015. Myrosinase-dependent and -independent formation and control of  
801 isothiocyanate products of glucosinolate hydrolysis. Front Plant Sci 6:831.

802 31. Liou CS, Sirk SJ, Diaz CAC, Klein AP, Fischer CR, Higginbottom SK, Erez A, Donia MS,  
803 Sonnenburg JL, Sattely ES. 2020. A Metabolic Pathway for Activation of Dietary  
804 Glucosinolates by a Human Gut Symbiont. Cell 180:717–728.e19.

805 32. Elfoul L, Rabot S, Khelifa N, Quinsac A, Duguay A, Rimbault A. 2001. Formation of allyl  
806 isothiocyanate from sinigrin in the digestive tract of rats monoassociated with a human  
807 colonic strain of *Bacteroides thetaiotaomicron*. FEMS Microbiol Lett 197:99–103.

808 33. Singh RK, Chang H-W, Yan D, Lee KM, Ucmak D, Wong K, Abrouk M, Farahnik B,  
809 Nakamura M, Zhu TH, Bhutani T, Liao W. 2017. Influence of diet on the gut microbiome  
810 and implications for human health. J Transl Med 15:73.

811 34. Johnson AJ, Vangay P, Al-Ghalith GA, Hillmann BM, Ward TL, Shields-Cutler RR, Kim  
812 AD, Shmagel AK, Syed AN, Personalized Microbiome Class Students, Walter J, Menon R,  
813 Koecher K, Knights D. 2019. Daily Sampling Reveals Personalized Diet-Microbiome  
814 Associations in Humans. Cell Host Microbe 25:789–802.e5.

815 35. Amato KR, Arrieta M-C, Azad MB, Bailey MT, Broussard JL, Bruggeling CE, Claud EC,  
816 Costello EK, Davenport ER, Dutilh BE, Swain Ewald HA, Ewald P, Hanlon EC, Julion W,

817 Keshavarzian A, Maurice CF, Miller GE, Preidis GA, Segurel L, Singer B, Subramanian S,

818 Zhao L, Kuzawa CW. 2021. The human gut microbiome and health inequities. *Proc Natl*

819 *Acad Sci U S A* 118:e2017947118.

820 36. Tropini C, Earle KA, Huang KC, Sonnenburg JL. 2017. The Gut Microbiome: Connecting

821 Spatial Organization to Function. *Cell Host Microbe* 21:433–442.

822 37. Hillman ET, Lu H, Yao T, Nakatsu CH. 2017. Microbial Ecology along the Gastrointestinal

823 Tract. *Microbes Environ* 32:300–313.

824 38. Lynch SV, Pedersen O. 2016. The Human Intestinal Microbiome in Health and Disease. *N*

825 *Engl J Med* 375:2369–2379.

826 39. Press AG, Hauptmann IA, Hauptmann L, Fuchs B, Fuchs M, Ewe K, Ramadori G. 1998.

827 Gastrointestinal pH profiles in patients with inflammatory bowel disease. *Aliment*

828 *Pharmacol Ther* 12:673–678.

829 40. Compare D, Pica L, Rocco A, De Giorgi F, Cuomo R, Sarnelli G, Romano M, Nardone G.

830 2011. Effects of long-term PPI treatment on producing bowel symptoms and SIBO.

831 European Journal of Clinical Investigation <https://doi.org/10.1111/j.1365-2362.2010.02419.x>.

833 41. Swidsinski A, Ladhoff A, Pernthaler A, Swidsinski S, Loening-Baucke V, Ortner M, Weber

834 J, Hoffmann U, Schreiber S, Dietel M, Lochs H. 2002. Mucosal flora in inflammatory

835 bowel disease. *Gastroenterology* 122:44–54.

836 42. Gevers D, Kugathasan S, Denson LA, Vázquez-Baeza Y, Van Treuren W, Ren B, Schwager

837 E, Knights D, Song SJ, Yassour M, Morgan XC, Kostic AD, Luo C, González A,  
838 McDonald D, Haberman Y, Walters T, Baker S, Rosh J, Stephens M, Heyman M,  
839 Markowitz J, Baldassano R, Griffiths A, Sylvester F, Mack D, Kim S, Crandall W, Hyams  
840 J, Huttenhower C, Knight R, Xavier RJ. 2014. The treatment-naive microbiome in new-  
841 onset Crohn's disease. *Cell Host Microbe* 15:382–392.

842 43. Kozik AJ, Nakatsu CH, Chun H, Jones-Hall YL. 2019. Comparison of the fecal, cecal, and  
843 mucus microbiome in male and female mice after TNBS-induced colitis. *PLoS One*  
844 14:e0225079.

845 44. Lai R-H, Miller MJ, Jeffery E. 2010. Glucoraphanin hydrolysis by microbiota in the rat  
846 cecum results in sulforaphane absorption. *Food Funct* 1:161–166.

847 45. Li F, Hullar MAJ, Beresford SAA, Lampe JW. 2011. Variation of glucoraphanin  
848 metabolism in vivo and ex vivo by human gut bacteria. *Br J Nutr* 106:408–416.

849 46. Eichele DD, Kharbanda KK. 2017. Dextran sodium sulfate colitis murine model: An  
850 indispensable tool for advancing our understanding of inflammatory bowel diseases  
851 pathogenesis. *World J Gastroenterol* 23:6016–6029.

852 47. Okayasu I, Hatakeyama S, Yamada M, Ohkusa T, Inagaki Y, Nakaya R. 1990. A novel  
853 method in the induction of reliable experimental acute and chronic ulcerative colitis in mice.  
854 *Gastroenterology* 98:694–702.

855 48. Wirtz S, Popp V, Kindermann M, Gerlach K, Weigmann B, Fichtner-Feigl S, Neurath MF.  
856 2017. Chemically induced mouse models of acute and chronic intestinal inflammation. *Nat*  
857 *Protoc* 12:1295–1309.

858 49. Poritz LS, Garver KI, Green C, Fitzpatrick L, Ruggiero F, Koltun WA. 2007. Loss of the  
859 tight junction protein ZO-1 in dextran sulfate sodium induced colitis. *J Surg Res* 140:12–19.

860 50. Chassaing B, Aitken JD, Malleshappa M, Vijay-Kumar M. 2014. Dextran sulfate sodium  
861 (DSS)-induced colitis in mice. *Curr Protoc Immunol* 104:15.25.1–15.25.14.

862 51. Araki A, Kanai T, Ishikura T, Makita S, Uraushihara K, Iiyama R, Totsuka T, Takeda K,  
863 Akira S, Watanabe M. 2005. MyD88-deficient mice develop severe intestinal inflammation  
864 in dextran sodium sulfate colitis. *J Gastroenterol* 40:16–23.

865 52. Dieleman LA, Ridwan BU, Tennyson GS, Beagley KW, Bucy RP, Elson CO. 1994.  
866 Dextran sulfate sodium-induced colitis occurs in severe combined immunodeficient mice.  
867 *Gastroenterology* 107:1643–1652.

868 53. da Costa Goncalves F, Schneider N, Mello HF, Passos EP, da Rosa Paz AH. 2013.  
869 Characterization of Acute Murine Dextran Sodium Sulfate (DSS) Colitis: Severity of  
870 Inflammation is Dependent on the DSS Molecular Weight and Concentration. *Acta  
871 Scientiae Veterinari* 41:1–9.

872 54. Breynaert C, Dresselaers T, Cremer J, Van Steen K, Perrier C, Vermeire S, Rutgeerts P,  
873 Ceuppens J, Himmelreich U, Van Assche G. 2012. P024 Repeated cycles of DSS inducing a  
874 chronically relapsing inflammation: A novel model to study fibrosis using in vivo MRI T2  
875 relaxometry. *J Crohns Colitis* 6:S20.

876 55. Delage C, Taib T, Mamma C, Lerouet D, Besson VC. 2021. Traumatic Brain Injury: An  
877 Age-Dependent View of Post-Traumatic Neuroinflammation and Its Treatment.  
878 *Pharmaceutics* 13:1624.

879 56. Sikorska-Zimny K, Beneduce L. 2021. The Metabolism of Glucosinolates by Gut  
880 Microbiota. *Nutrients* 13:2750.

881 57. Luang-In V, Narbad A, Cebeci F, Bennett M, Rossiter JT. 2015. Identification of Proteins  
882 Possibly Involved in Glucosinolate Metabolism in *L. agilis* R16 and *E. coli* VL8. *Protein J*  
883 34:135–146.

884 58. Chénard T, Malick M, Dubé J, Massé E. 2020. The influence of blood on the human gut  
885 microbiome. *BMC Microbiol* 20:44.

886 59. Cafiero C, Re A, Pisconti S, Trombetti M, Perri M, Colosimo M, D'Amato G, Gallelli L,  
887 Cannataro R, Molinario C, Fazio A, Caroleo MC, Cione E. 2020. Dysbiosis in intestinal  
888 microbiome linked to fecal blood determined by direct hybridization. *3 Biotech* 10:358.

889 60. Mähler M, Bristol IJ, Leiter EH, Workman AE, Birkenmeier EH, Elson CO, Sundberg JP.  
890 1998. Differential susceptibility of inbred mouse strains to dextran sulfate sodium-induced  
891 colitis. *Am J Physiol* 274:G544–51.

892 61. Bábíčková J, Tóthová L, Lengyelová E, Bartoňová A, Hodosy J, Gardlík R, Celec P. 2015.  
893 Sex Differences in Experimentally Induced Colitis in Mice: a Role for Estrogens.  
894 *Inflammation* 38:1996–2006.

895 62. Goodman WA, Havran HL, Quereshy HA, Kuang S, De Salvo C, Pizarro TT. 2018.  
896 Estrogen Receptor  $\alpha$  Loss-of-Function Protects Female Mice From DSS-Induced  
897 Experimental Colitis. *Cell Mol Gastroenterol Hepatol* 5:630–633.e1.

898 63. Letourneau J, Holmes ZC, Dallow EP, Durand HK, Jiang S, Carrion VM, Gupta SK,

899 Mincey AC, Muehlbauer MJ, Bain JR, David LA. 2022. Ecological memory of prior  
900 nutrient exposure in the human gut microbiome. *ISME J* 16:2479–2490.

901 64. Yagishita Y, Fahey JW, Dinkova-Kostova AT, Kensler TW. 2019. Broccoli or  
902 Sulforaphane: Is It the Source or Dose That Matters? *Molecules* 24:3593.

903 65. Stackebrandt E, Kramer I, Swiderski J, Hippe H. 1999. Phylogenetic basis for a taxonomic  
904 dissection of the genus *Clostridium*. *FEMS Immunol Med Microbiol* 24:253–258.

905 66. Uzal FA, McClane BA, Cheung JK, Theoret J, Garcia JP, Moore RJ, Rood JI. 2015. Animal  
906 models to study the pathogenesis of human and animal *Clostridium perfringens* infections.  
907 *Vet Microbiol* 179:23–33.

908 67. Chen H, Ma X, Liu Y, Ma L, Chen Z, Lin X, Si L, Ma X, Chen X. 2019. Gut Microbiota  
909 Interventions With *Clostridium butyricum* and Norfloxacin Modulate Immune Response in  
910 Experimental Autoimmune Encephalomyelitis Mice. *Front Immunol* 10:1662.

911 68. Shahinuzzaman M, Raychaudhuri S, Fan S, Obanda DN. 2021. Kale Attenuates  
912 Inflammation and Modulates Gut Microbial Composition and Function in C57BL/6J Mice  
913 with Diet-Induced Obesity. *Microorganisms* 9:238.

914 69. Ju T, Kong JY, Stothard P, Willing BP. 2019. Defining the role of *Parasutterella*, a  
915 previously uncharacterized member of the core gut microbiota. *ISME J* 13:1520–1534.

916 70. Hubbard TD, Murray IA, Nichols RG, Cassel K, Podolsky M, Kuzu G, Tian Y, Smith P,  
917 Kennett MJ, Patterson AD, Perdew GH. 2017. Dietary Broccoli Impacts Microbial  
918 Community Structure and Attenuates Chemically Induced Colitis in Mice in an Ah receptor

919 dependent manner. *J Funct Foods* 37:685–698.

920 71. Antonson AM, Evans MV, Galley JD, Chen HJ, Rajasekera TA, Lammers SM, Hale VL,  
921 Bailey MT, Gur TL. 2020. Unique maternal immune and functional microbial profiles  
922 during prenatal stress. *Sci Rep* 10:20288.

923 72. Huarte-Mendicoa JC, Astiasarán I, Bello J. 1997. Nitrate and nitrite levels in fresh and  
924 frozen broccoli. Effect of freezing and cooking. *Food Chem* 58:39–42.

925 73. Araki Y, Mukaisho K, Sugihara H, Fujiyama Y, Hattori T. 2010. *Proteus mirabilis* sp.  
926 intestinal microflora grow in a dextran sulfate sodium-rich environment. *Int J Mol Med*  
927 25:203–208.

928 74. Chang C-S, Liao Y-C, Huang C-T, Lin C-M, Cheung CHY, Ruan J-W, Yu W-H, Tsai Y-T,  
929 Lin I-J, Huang C-H, Liou J-S, Chou Y-H, Chien H-J, Chuang H-L, Juan H-F, Huang H-C,  
930 Chan H-L, Liao Y-C, Tang S-C, Su Y-W, Tan T-H, Bäumler AJ, Kao C-Y. 2021.  
931 Identification of a gut microbiota member that ameliorates DSS-induced colitis in intestinal  
932 barrier enhanced Dusp6-deficient mice. *Cell Rep* 37:110016.

933 75. Khan I, Bai Y, Ullah N, Liu G, Rajoka MSR, Zhang C. 2022. Differential Susceptibility of  
934 the Gut Microbiota to DSS Treatment Interferes in the Conserved Microbiome Association  
935 in Mouse Models of Colitis and Is Related to the Initial Gut Microbiota Difference.  
936 *Advanced Gut & Microbiome Research* 2022:7813278.

937 76. Gibbons SM. 2020. Keystone taxa indispensable for microbiome recovery. *Nature*  
938 *Microbiology* 5:1067–1068.

939 77. Duvallet C, Gibbons SM, Gurry T, Irizarry RA, Alm EJ. 2017. Meta-analysis of gut  
940 microbiome studies identifies disease-specific and shared responses. *Nat Commun* 8:1784.

941 78. Walters WA, Xu Z, Knight R. 2014. Meta-analyses of human gut microbes associated with  
942 obesity and IBD. *FEBS Lett* 588:4223–4233.

943 79. Han YW. 2015. *Fusobacterium nucleatum*: a commensal-turned pathogen. *Curr Opin*  
944 *Microbiol* 23:141–147.

945 80. Gu M, Samuelson DR, de la Rua NM, Charles TP, Taylor CM, Luo M, Siggins RW,  
946 Shellito JE, Welsh DA. 2022. Host innate and adaptive immunity shapes the gut microbiota  
947 biogeography. *Microbiol Immunol* 66:330–341.

948 81. Suzuki TA, Nachman MW. 2016. Spatial Heterogeneity of Gut Microbial Composition  
949 along the Gastrointestinal Tract in Natural Populations of House Mice. *PLoS One*  
950 11:e0163720.

951 82. Wu S, Zhang B, Liu Y, Suo X, Li H. 2018. Influence of surface topography on bacterial  
952 adhesion: A review (Review). *Biointerphases* 13:060801.

953 83. Stenman LK, Holma R, Forsgård R, Gylling H, Korpela R. 2013. Higher fecal bile acid  
954 hydrophobicity is associated with exacerbation of dextran sodium sulfate colitis in mice. *J*  
955 *Nutr* 143:1691–1697.

956 84. Fahey JW, Smilovitz Burak J, Evans D. 2022. Sprout microbial safety: A reappraisal after a  
957 quarter-century. *Food Frontiers* 1–7.

958 85. Rao M, Afshin A, Singh G, Mozaffarian D. 2013. Do healthier foods and diet patterns cost

959 more than less healthy options? A systematic review and meta-analysis. *BMJ Open*  
960 3:e004277.

961 86. Economic Research Service. Food Access Research Atlas. US Department of Agriculture.  
962 <https://www.ers.usda.gov/data/fooddesert>. Retrieved 22 April 2022.

963 87. Wedick NM, Ma Y, Olendzki BC, Procter-Gray E, Cheng J, Kane KJ, Ockene IS, Pagoto  
964 SL, Land TG, Li W. 2015. Access to healthy food stores modifies effect of a dietary  
965 intervention. *Am J Prev Med* 48:309–317.

966 88. Baker EA, Shootman M, Barnidge E, Kelly C. 2006. The role of race and poverty in access  
967 to foods that enable individuals to adhere to dietary guidelines. *Prev Chronic Dis* 3:A76.

968 89. Taghipour N, Molaei M, Mosaffa N, Rostami-Nejad M, Asadzadeh Aghdaei H, Anissian A,  
969 Azimzadeh P, Zali MR. 2016. An experimental model of colitis induced by dextran sulfate  
970 sodium from acute progresses to chronicity in C57BL/6: correlation between conditions of  
971 mice and the environment. *Gastroenterol Hepatol Bed Bench* 9:45–52.

972 90. Chassaing B, Srinivasan G, Delgado MA, Young AN, Gewirtz AT, Vijay-Kumar M. 2012.  
973 Fecal Lipocalin 2, a Sensitive and Broadly Dynamic Non-Invasive Biomarker for Intestinal  
974 Inflammation. *PLoS One* 7:e44328.

975 91. Nocker A, Sossa-Fernandez P, Burr MD, Camper AK. 2007. Use of propidium monoazide  
976 for live/dead distinction in microbial ecology. *Appl Environ Microbiol* 73:5111–5117.

977 92. Pedersen EJ, Miller DL, Simpson GL, Ross N. 2018. Hierarchical generalized additive  
978 models: an introduction with mgcv. *PeerJ Preprint* e27320v1.

979 93. Oksanen J, Guillaume Blanchet F, Friendly M, Kindt R, Legendre P, McGlinn D, Minchin  
980 PR, O'Hara RB, Simpson GL, Solymos P, Stevens MHH, Szoecs E, Wagner H. 2020.  
981 Vegan: Community Ecology Package (2.5-7). [https://cran.r-  
982 project.org/web/packages/vegan/vignettes/diversity-vegan.pdf](https://cran.r-project.org/web/packages/vegan/vignettes/diversity-vegan.pdf).

983 94. Archer E. 2022. rfpermutation: Estimate Permutation p-Values for Random Forest Importance  
984 Metrics (2.5.1). <https://github.com/EricArcher/rfPermutation>.

985 95. Wickham H. 2016. ggplot2: Elegant graphics for Data Analysis. Springer Publishing  
986 Company, New York. <https://dl.acm.org/citation.cfm?id=1795559>.

987 96. Kassambara A. 2022. ggpubr: “ggplot2” based publication ready plots (0.1.7).  
988 <https://rpkgs.datanovia.com/ggpubr/>.

989 97. Knights D, Kuczynski J, Charlson ES, Zaneveld J, Mozer MC, Collman RG, Bushman FD,  
990 Knight R, Kelley ST. 2011. Bayesian community-wide culture-independent microbial  
991 source tracking. Nat Methods 8:761–763.

992 98. Galey M. 2021. Mi-Seq Analysis. GitHub. <https://mgaley-004.github.io/MiSeq-Analysis/Tutorials/SourceSink.html>, <https://github.com/mgaley-004/MiSeq-Analysis>.  
993 Retrieved 7 December 2022.

995